Incorporating *Phaeocystis* into a Southern Ocean ecosystem model

Shanlin Wang[1] and J. Keith Moore[1]

Received 17 September 2009; revised 26 August 2010; accepted 30 November 2010; published 28 January 2011.

[1] *Phaeocystis antarctica* is an important phytoplankton species in the Southern Ocean. We incorporated *P. antarctica* into the biogeochemical elemental cycling ocean model to study Southern Ocean ecosystem dynamics and biogeochemistry. The optimum values of ecological parameters for *Phaeocystis* were sought through synthesizing laboratory and field observations, and the model output was evaluated with observed chlorophyll *a*, carbon biomass, and nutrient distributions. Several factors have been proposed to control Southern Ocean ecosystem structure, including light adaptation, iron uptake capability, and loss processes. Optimum simulation results were obtained when *P. antarctica* had a relatively high α (P-I curve initial slope) value and a higher half-saturation constant for iron uptake than other phytoplankton. Simulation results suggested that *P. antarctica* had a competitive advantage under low irradiance levels, especially in the Ross Sea and Weddell Sea. However, the distributions of *P. antarctica* and diatoms were also strongly influenced by iron availability. Although grazing rates had an influence on total biomass, our simulations did not show a strong influence of grazing pressure in the competition between *P. antarctica* and diatoms. However, limited observations and the relative simplicity of zooplankton in our model suggest further research is needed. Overall, *P. antarctica* contributed ~13% of annual primary production and ~19% of sinking carbon export in the Southern Ocean (>40°S) in our best case simulation. At higher latitudes (>60°S) *P. antarctica* accounts for ~23% of annual primary production and ~30% of sinking carbon export.

Citation: Wang, S., and J. K. Moore (2011), Incorporating *Phaeocystis* into a Southern Ocean ecosystem model, *J. Geophys. Res.*, *116*, C01019, doi:10.1029/2009JC005817.

1. Introduction

[2] The Southern Ocean, the largest of three high-nutrient, low-chlorophyll (HNLC) regions, is an important component of the global ocean. The concentrations of macronutrients (nitrate, phosphate, and silicic acid) are generally high, while chlorophyll concentrations are relatively low. The Southern Ocean plays key roles in global marine biogeochemical cycles and climate change. This region accounts for a large fraction of the carbon inventory of global anthropogenic CO_2 [*Gruber et al.*, 2009; *Sabine et al.*, 2004; *Takahashi et al.*, 2002]. Antarctic Bottom Water (AABW), Antarctic Intermediate Water (AAIW), and Subantarctic mode water (SAMW) form in this region. AABW brings a large amount of nutrient-rich water to the deep ocean, which significantly affects chemical properties in the global deep oceans. AAIW exports nutrients into the thermocline, which is a key nutrient source for equatorial upwelling regions. Therefore, the ecosystem dynamics and biogeochemical cycles (N, P, C, Si, and Fe) in the Southern Ocean influence the air-sea CO_2 balance and oceanic export production not only in this region but globally.

[3] Phytoplankton are key drivers of biogeochemical cycles. The community composition has a strong influence on trophic pathways, biogeochemical processes, and fluxes from surface waters to the deep ocean. Since the element fluxes among the atmosphere, the upper ocean, and the ocean interior are crucially dependent on oceanic ecosystems, especially several key groups of phytoplankton, the simulations of biogeochemical cycles are highly related to the representativeness of functional groups in the model. Diatoms, which build their frustules with silicon, are the major blooming phytoplankton in the Southern Ocean. However, *Phaeocystis* has been recognized as one of the most important phytoplankton in the Southern Ocean in recent years, sometimes dominating the community during blooms [*DiTullio et al.*, 2000; *Feng et al.*, 2010; *Poulton et al.*, 2007; *Smith and Asper*, 2001].

[4] *Phaeocystis* species are common in the global ocean [*Schoemann et al.*, 2005]. It mainly has two morphotypes: solitary cells and mucilaginous colonies. There are three common *Phaeocystis* blooming species, *P. pouchetii*, *P. antarctica*, *P. globosa*. Generally, *P. antarctica* is found in cool Antarctic waters. *Phaeocystis* form blooms in nutrient-enriched areas mainly as colonies [*Schoemann et al.*, 2005]. When solitary cells of *Phaeocystis* form gelatinous colonies, the growth rate is higher than the growth rate of free-living cells [*Veldhuis et al.*, 2005] and the defensive ability against grazers, viruses, and other pathogens also improves due to the increased size and the protection of gelatinous periphery

[1]Department of Earth System Science, University of California, Irvine, California, USA.

0148-0227/11/2009JC005817

surrounding *Phaeocystis* cells [*Hamm et al.*, 1999]. The particular physiology of *Phaeocystis* can cause unusual elemental composition and stoichiometry, especially for mucilaginous colonies [*Mathot et al.*, 2000; *Schoemann et al.*, 2005; *Solomon et al.*, 2003].

[5] Field investigations have found massive *Phaeocystis* colony blooms in Antarctic waters in early spring, which terminate with the depletion of nutrients, for example, in the coastal regions of the Ross Sea, the Weddell Sea, and around the Crozet Plateau [*Dennett et al.*, 2001; *Fryxell and Kendrick*, 1988; *Mathot et al.*, 2000; *Poulton et al.*, 2007]. In those areas, *Phaeocystis* may be capable of adaptation to low-light intensities, even in the presence of sea ice cover [*Palmisano et al.*, 1986; *Tang et al.*, 2009]. Frequent blooms make *Phaeocystis* very likely an important contributor to primary production and the carbon cycle. However, exactly how *Phaeocystis* mediates ecosystem community structure and biogeochemical fluxes is poorly understood. How the phytoplankton community will react to climate change is even less understood. During the past two decades, considerable research efforts have been made to study the Southern Ocean, including research cruises in JGOFS (Joint Global Ocean Flux Study), artificial and natural iron fertilization experiments, and other projects [*Coale et al.*, 2003; *de Baar et al.*, 2005; *Dennett et al.*, 2001; *Moore et al.*, 2007; *Poulton et al.*, 2007]. Those scientific efforts provide a great opportunity to improve modeling studies of *P. antarctica* and its role in the marine ecosystem, which can better explain the controlling mechanisms in the competition between different phytoplankton groups, and the interactions between biogeochemical cycles and Southern Ocean ecosystem dynamics.

[6] Net growth and biomass accumulation of different phytoplankton groups are key controls on ecosystem structure and the competition between diatoms and *Phaeocystis*. The accumulation of biomass is determined by the imbalance between growth and loss of phytoplankton. However, the processes governing phytoplankton community composition are complex. For example, the Ross Sea is often widely dominated by two taxa, diatoms, and *P. antarctica*. Generally, some observed blooms showed distinct spatial and temporal regimes of those two taxa [*Arrigo et al.*, 1999; *Peloquin and Smith*, 2007]. It was reported by *Smith et al.* [1999] that the growth rate of diatom assemblage averaged 0.10 day^{-1} in early growing season, while the growth rate of *P. antarctica* dominant assemblage was 0.41 day^{-1} throughout the growth season, which was much higher than the diatoms in 1994. Yet diatoms became more abundant even with lower growth rates during summer [*Smith et al.*, 1999]. The main factors which have been proposed to control phytoplankton competition, are light adaptation, iron requirements and uptake capability, and grazing and other loss processes [*Peloquin and Smith*, 2007; *Poulton et al.*, 2007; *Smith et al.*, 1999; *Tang et al.*, 2009].

[7] In previous studies, the conclusions related to the factors controlling the phytoplankton community structure were somewhat inconsistent. In the Research on Ocean-Atmosphere Variability and Ecosystem Response in the Ross Sea (ROAVERRS) field study during 1996–1997, *Arrigo et al.* [1999] found *P. antarctica* dominated the southernmost area of the Ross Sea, where the mixed layer depths were deeper. They suggested the different distributions of *Phaeocystis* and diatoms were because *Phaeocystis* is better adapted to lower irradiance levels. *Arrigo et al.* [2003] suggested that light was the major controller on regulating phytoplankton community composition, while Fe availability played little role in determining ecosystem structure in the Ross Sea. Some other field observations and experiments also confirmed the large contribution of *Phaeocystis* in low-light subsurface waters [*Mangoni et al.*, 2004; *Shields and Smith*, 2009] and the importance of diatoms in stratified waters [*Alvain et al.*, 2008].

[8] During two cruises of the RVIB *Nathaniel B. Palmer* between 1994 and 1996, accessory pigment measurements suggested that *P. antarctica* were able to grow and accumulate under low, in situ irradiance level. The fast growth of *Phaeocystis* appeared earlier in spring than diatoms. But the variations of mixed layer depth were not always correlated with the dominance of diatoms and/or *Phaeocystis* [*Smith and Asper*, 2001]. They suggested that the spatial distributions of diatoms and *Phaeocystis* were often not distinct [*Smith and Asper*, 2001].

[9] Results from incubation experiments supported the hypothesis that *Phaeocystis* has higher growth rate at lower irradiance than diatoms [*Moore et al.*, 2007]. However, *Moore et al.* [2007] also found a strong response of *Phaeocystis* to Fe amendment. Furthermore, the results of iron addition experiments in the Ross Sea and Antarctic Circumpolar Current along 170°W showed that *Phaeocystis* responded the most strongly to iron addition, and the iron addition resulted in a switch of the community structure from diatoms to *Phaeocystis* [*Coale et al.*, 2003]. This suggests that the abundance of iron may be also an important factor controlling the distribution of *Phaeocystis* and diatoms.

[10] *Phaeocystis* and diatoms can have very different stoichiometry and export processes [*Arrigo et al.*, 1999; *Asper and Smith*, 1999]. The N/P removal ratios of *P. antarctica* were generally found markedly higher than the N/P removal ratios of diatoms, although the amplitude of the differences remained in a wide range [*Arrigo et al.*, 1999; *Smith and Asper*, 2001]. *P. antarctica* can have much higher carbon to phosphorus ratios compared to diatoms [*Arrigo et al.*, 1999]. Also, the C: N of *P. antarctica* colonies can be significantly higher than single cells due to increased production of the mucilaginous matrix during blooms [*Solomon et al.*, 2003]. Nutrient-replete *Phaeocystis* tend to have stoichiometry closer to the Redfield ratio [*Schoemann et al.*, 2005]. The capacity of the carbon biological pump in the Southern Ocean may significantly change when phytoplankton community structure shifts between *Phaeocystis* and diatoms, which may happen due to climate change. Hence, it is necessary to better understand controlling factors on the competition between diatoms and *P. antarctica* and the contributions of *Phaeocystis* to biogeochemical cycles and primary production in the Southern Ocean.

[11] *Phaeocystis* has been included in several models in recent several years. For Southern Ocean research, *Arrigo et al.* [2003] and *Worthen and Arrigo* [2004] developed a regional scale coupled ocean-ecosystem model, the Ross Sea Coupled Ice and Ocean (CIAO) model. This model included six biological variables in total, two phytoplankton groups (diatoms and *P. antarctica*), two nutrients (nitrate and iron), detritus, and one zooplankton group. Iron impacts on

phytoplankton dynamics, ecosystem and primary production, and the interannual variation in air-sea CO_2 flux in the Ross Sea are investigated with this model [*Arrigo et al.*, 2003; *Arrigo and Van Dijken*, 2007; *Tagliabue and Arrigo*, 2005, 2006; *Worthen and Arrigo*, 2004]. *Pasquer et al.* [2005] reported on simulations with the coupled Sea Water Microbial Community model (SWAMCO-4) and a one-dimensional (1-D) physical model of the sea ice and water column. This SWAMCO-4 model includes diatoms, small phytoplankton ($\leq$20 μm) belonging to other taxonomic groups, coccolithophorids, and *Phaeocystis*. Export production and air-sea CO_2 flux were simulated and compared with three different JGOFS site observations [*Pasquer et al.*, 2005]. A similar model was used to study the mechanisms regulating the succession of diatoms and *Phaeocystis* and nutrient cycling in the Belgian coastal zone [*Lancelot et al.*, 2005].

[12] In this study, the ocean biogeochemical elemental cycling (BEC) model was used to simulate ecosystem dynamics in the Southern Ocean. *P. antarctica* was added as an additional phytoplankton functional group, and different ecological parameters for *Phaeocystis* were tuned based on field observations and laboratory results. With the optimized parameter set, we examined the key factors controlling the growth and distribution of *Phaeocystis*. Furthermore, we examined the contributions of different phytoplankton groups to carbon and nutrient cycling in the Southern Ocean.

2. Methods

[13] The BEC model is a coupled ocean biogeochemical/ecosystem model [*Moore et al.*, 2002, 2004], which runs within the three-dimensional ocean circulation component of the National Center for Atmospheric Research (NCAR) Community Climate System Model 3.1 (CCSM3) at relatively coarse resolution [*Collins et al.*, 2006; *Yeager et al.*, 2006]. The model includes 25 vertical levels with 8 levels in the upper 103 m. Also, it has 100 × 116 horizontal grid points. The longitudinal resolution is 3.6° and the latitudinal resolution varies in the range of 0.9°–2.0° with finer resolution near the equator. The BEC model is forced with the NCEP/NCAR meteorological reanalysis climatology data and the satellite-based estimates climatological surface ice cover for the current study [*Large and Yeager*, 2004]. Dust deposition is from the climatology of *Luo et al.* [2003]. Our focus here is on the Southern Ocean (>40°S).

[14] The wind speed-mixing relation is adjusted to better match the observed mixed layer depths in the Southern Ocean [*de Boyer Montégut et al.*, 2004]. This is relevant because mixed layer depths tend to be too shallow in CCSM3.1 [*Doney et al.*, 2004, 2009]. The bias in monthly mean Southern Ocean mixed layer depth is −18 m in the standard CCSM3.1, but declines to +2 m in our simulations, when compared with the observational estimates from *de Boyer Montégut et al.* [2004]. These mixed layer biases and their impacts on the marine ecosystems and biogeochemistry have been discussed previously by *Doney et al.* [2009]. Mean mixed layer depths in this study are in much better agreement with the observations than in our previous studies. However, some biases remain, mixed layer depths in the core of the ACC tend to be too deep early in the growing season (November), and somewhat shallower than observed at the highest latitudes during summer months (December, January).

2.1. BEC Model Description

[15] The ecosystem component consisted of 13 main compartments: five phytoplankton functional groups, dissolved organic matter (DOM), sinking particles, one zooplankton group, and several key nutrients (nitrate, ammonium, phosphate, iron, and dissolved silicon) [*Moore et al.*, 2004]. The phytoplankton functional groups were diatoms, diazotrophs, small phytoplankton, coccolithophores, and *Phaeocystis*. The most important groups in our study area are diatoms, *Phaeocystis*, and small phytoplankton. Diatoms, representing larger phytoplankton, often dominate phytoplankton blooms and sinking carbon export out of surface waters. Small phytoplankton ($\leq$20 μm, belonging to other taxonomic groups) can thrive under low nutrient conditions. *Phaeocystis*, a competitive blooming species, was added to BEC model as an additional phytoplankton functional group in this study.

[16] The growth rates of phytoplankton groups are set to reduce proportionally under nutrient stress using Michaelis-Menten nutrient uptake kinetics [*Moore et al.*, 2002]. Detailed model parameters and equations are given by *Moore et al.* [2002, 2004]. Taking diatoms as example, several equations are listed here to illustrate some basic processes in the model. The light, nutrient, and temperature dependencies of phytoplankton growth rate are modeled multiplicatively as shown in equations (1) and (2). Thus, the balanced growth rates for phytoplankton groups are allowed to be colimited by light, temperature, and nutrient availabilities [*Moore et al.*, 2004]

$$\text{photoC\_diat} = \text{PCphoto\_diat} * \text{diatC} \quad (1)$$

$$\text{PCphoto\_diat} = \text{PCref} * \text{f\_nut} * \text{Tfunc} * \text{light\_lim}. \quad (2)$$

The photoC_diat is diatom C fixation (mmol C/m^3/d). PCphoto_diat is diatom C-specific rate of photosynthesis (1/day), which is calculated by PCref (the maximum phytoplankton C-specific growth rate, per day), f_nut (the nutrient growth limitation factor), Tfunc (the temperature function used to scale biological rates, with a Q10 value of 2.0) and light_lim (the light limitation factor). The diatC term is diatom carbon biomass. The f_nut term is determined by the minimum of all relative nutrient uptake values, f_fe_diat, f_si_diat, f_p_diat, and f_nit_diat. For example, the relative iron uptake rate is determined as f_fe_diat = Fe_loc/(Fe_loc + diat_kFe). Fe_loc and diat_kFe are local Fe concentration and diatom iron uptake half-saturation coefficient (nM), respectively. The light limitation factor is calculated as follows [*Geider et al.*, 1998]:

$$\text{light\_lim} = 1.0 - \exp((-1.0 * \text{alphachl} * \text{thetaC\_diat} * \text{Epar})/\text{PCmax} \quad (3)$$

$$\text{PCmax} = \text{PCref} * \text{f\_nut} * \text{Tfunc}. \quad (4)$$

The thetaC_diat is diatom Chl/C ratio (mg/mmol); alphachl is chlorophyll specific initial slope of P versus I curve for diatoms, unit is mmol C m^2/mg ChlWd; and Epar is the average PAR over each model layer (W/m^2), which is converted as a constant fraction (0.45) of incident shortwave radiation and depends on absorption by water and chlorophyll in subsurface waters [*Moore et al.*, 2002].

[17] The growth limitation factor for phytoplankton at each location is determined by the most limiting factor among all nutrients and light availability. Then the nutrient uptake by diatoms is calculated based on diatoms C fixation, i.e., photoFe_diat = photoC_diat * gQfe_diat, where photoFe_diat is diatom iron uptake and gQfe_diat is diatom fe/C ratio for growth. Similar equations are used for the other nutrients.

[18] As shown in equations (5) and (6), photoadaptation is described as a variable chlorophyll to nitrogen ratio based on the model of *Geider et al.* [1998]. Chlorophyll synthesis is regulated by the balance between photosynthetic carbon fixation and light absorption and assumed to be proportional to nitrogen uptake. Nitrogen uptake reflects the need for the synthesis of proteins used in light harvesting complexes and elsewhere in the photosynthetic system [*Geider et al.*, 1998; *Moore et al.*, 2002]. The maximum of Chl/N ratio has the highest value for diatoms (a value of 4.0 mg $mmol^{-1}$) and a lower value for *Phaeocystis* and small phytoplankton (a value of 2.5 mg $mmol^{-1}$)

$$\text{pChl\_diat} = \text{thetaNmax} * \text{PCphoto\_diat}/(\text{alphaChl} * \text{thetaC\_diat} * \text{Epar}) \quad (5)$$

$$\text{photoaclim\_diat} = (((\text{pChl\_diat} * \text{Vnc\_diat})/\text{thetaC\_diat}) - \text{Rref}) * \text{diatChl}. \quad (6)$$

The pChl_diat is diatom chlorophyll synthesis term, thetaNmax is the maximum Chl/N ratio, photoaclim_diat is the change in diatom chlorophyll due to photoadaptation, Vnc_diat is total nitrogen uptake by diatoms, and diatChl is diatom chlorophyll.

[19] The losses of phytoplankton are natural mortality/respiration, zooplankton grazing, and phytoplankton aggregation. Parameters values for grazing loss are set based on different features of phytoplankton groups. In the BEC model, the single zooplankton group represents both small zooplankton and large zooplankton. The grazing pressure on phytoplankton varies for different groups. The maximum of grazing rate is set for small phytoplankton, and a lower grazing rate is set for diatoms and *P. antarctica* colonies, making blooms more likely. The C_loss_thres is a biomass carbon threshold at which losses go to zero (mmol C/m^3), necessary to maintain seed populations. The nongrazing mortality (diat_loss) is set at a constant value (mort) for small phytoplankton, diatoms, and *Phaeocystis*, scaled by the temperature function (equations (7) and (8)). Aggregation losses (e.g., diat_agg, the diatom aggregation loss) are a function of biomass according to quadratic equations, which are minimal when biomass is low and higher under bloom conditions (equation (9)). The mort2 is coefficient in quadratic mortality/aggregation term for small phytoplankton, diatoms, and *Phaeocystis* (1/d/((mmol C/m^3))

$$\text{Pprime} = \max(\text{diatC} - \text{C\_loss\_thres}, 0.0), \quad (7)$$

$$\text{diat\_loss} = \text{mort} * \text{Pprime} * \text{Tfunc}, \quad (8)$$

$$\text{diat\_agg} = \min((\text{agg\_rate\_max}) * \text{Pprime}, \text{mort2} * \text{Pprime} * \text{Pprime}). \quad (9)$$

Calcification was set with a base calcification rate of 5% of the photosynthetic carbon fixation of the small phytoplankton group and modified by functions of sea surface temperature and nutrient concentrations [*Moore et al.*, 2002]. Biogenic Si production is calculated by diatom carbon fixation rate and diatoms Si/C ratio for growth, which is a function of ambient nutrient concentrations (Fe and Si) [*Moore et al.*, 2002]. Ecosystem parameters are set based on field and laboratory data [*Moore et al.*, 2004]. Key parameters are listed in Table 1. The losses of phytoplankton and zooplankton enter detrital organic pools. Sinking detrital and mineral ballast pools instantly sink and remineralize at depth, and remineralization at depth is prescribed based on the mineral ballast model of *Armstrong et al.* [2002] (see *Moore et al.* [2004] for details). The initial distributions of nutrients are from the World Ocean Atlas 2001 database [*Conkright et al.*, 2002] and the GLODAP database [*Key et al.*, 2004]. The dissolved iron initialization is based on prior BEC model simulations by *Moore and Braucher* [2008]. Iron sources include both atmospheric dust deposition and sedimentary diffusion [*Moore and Braucher*, 2008]. Detailed description of the BEC model are given by *Moore et al.* [2004] and *Moore and Braucher* [2008].

2.2. Simulations of *Phaeocystis antarctica*

[20] Though there are multiple morphotypes in the *Phaeocystis* life cycle [*Rousseau et al.*, 1994], *Phaeocystis* blooms are mainly dominated by *P. antarctica* colonies in the Southern Ocean [*Schoemann et al.*, 2005]. We consider single cells of *P. antarctica* as a part of our small phytoplankton functional group and the biogeochemical parameters of the *Phaeocystis* group for nutrient uptake, light adaptation, biogeochemical cycling, and composition are mainly chosen according to the observed features of *P. antarctica* colonies. *Phaeocystis* colonies are assumed to be able to form where and when light, temperature, and nutrient concentrations can meet their needs. Thus we assume there is always a seed stock of solitary *Phaeocystis* cells present in Southern Ocean waters.

[21] The parameter values of photosynthetic properties, nutrient uptake, and stoichiometry were chosen based on the observational and laboratorial database [e.g., *Matrai et al.*, 1995; *Palmisano et al.*, 1986; *Schoemann et al.*, 2005; *van Hilst and Smith*, 2002; *van Leeuwe and Stefels*, 1998]. Physiological parameters of *P. antarctica* were collected from field observations and experimental work. The observed values of those parameters lay within relatively large ranges. A series of parameter values around the mean and median were tested with short-term simulations to determine optimal values. To examine model performance, we also compiled databases of monthly *Phaeocystis* and diatom carbon biomass in the Southern Ocean from published field observations (complete references and the carbon biomass database are given in the auxiliary material).[1] We collected carbon biomass of *P. antarctica* colonies and diatoms and cell abundances data of *P. antarctica* colonies. The cell densities were converted to carbon biomass based on cell carbon content using the value from *Mathot et al.* [2000] (see auxiliary material). Those carbon biomass distribution data

[1] Auxiliary materials are available at ftp://ftp.agu.org/apend/jc/2009jc005817.

Table 1. Key Parameters Used in the BEC Model[a]

Symbols	Values	Parameters
PCref[b]	3.0	C specific growth rates for diatoms, small phytoplankton and *Phaeocystis* (1/day)
sp_kNO3	0.5	half-saturation constant (*Ks*) value for small phytoplankton nitrate uptake
diat_kNO3	2.5	*Ks* value for diatom nitrate uptake (μM)
phaeo_kNO3	2.5	*Ks* value for *Phaeocystis* nitrate uptake (μM)
sp_kNH4	0.01	*Ks* value for small phytoplankton ammonium uptake (μM)
diat_kNH4	0.1	*Ks* value for diatom ammonium uptake (μM)
phaeo_kNH4	0.1	*Ks* value for *Phaeocystis* ammonium uptake (μM)
diat_kSiO3	1.0	*Ks* value for diatom silicate uptake (μM)
sp_PO4	0.01	*Ks* value for small phytoplankton phosphate uptake (μM)
diat_PO4	0.1	*Ks* value for diatom phosphate uptake (μM)
phaeo_PO4	0.1	*Ks* value for *Phaeocystis* phosphate uptake (μM)
sp_kFe	3.5×10^{-5}	*Ks* value for small phytoplankton iron uptake (nM)
diat_kFe	8×10^{-5}	*Ks* value for diatom iron uptake (nM)
phaeo_kFe	1.8×10^{-4}	*Ks* value for *Phaeocystis* iron uptake (nM)
alphaChlsp	0.28	initial slope of P versus I curve for small phytoplankton (mmol C m^2/mg Chl W d)
alphaChl	0.25	initial slope of P versus I curve for diatoms (mmol C m^2/mg Chl W d)
alphaChlphaeo	0.63	initial slope of P versus I curve for *Phaeocystis* (mmol C m^2/mg Chl W d)
thetaN_max_sp	2.5	maximum Chl/N ratio for small phytoplankton (mg/mmol)
thetaN_max_diat	4.0	maximum Chl/N ratio for diatoms (mg/mmol)
thetaN_max_phaeo	2.5	maximum Chl/N ratio for *Phaeocystis* (mg/mmol)
mort	0.17	nongrazing mortality term for small phytoplankton, diatoms and *Phaeocystis* (1/day)
agg_rate_max	0.75	maximum aggregation rate for small phytoplankton, diatoms and *Phaeocystis* (1/day)
agg_rate_min	0.01	minimum aggregation rate for small phytoplankton, diatoms and *Phaeocystis* (1/day)
mort2	0.0035	coefficient in quadratic mortality/aggregation term for small phytoplankton, diatoms and *Phaeocystis* (1/d/((mmol C/m^3))
z_umax[b]	3.1	maximum grazing rate on small phytoplankton (1/day)
diat_umax[b,c]	3.06~5.1	maximum grazing rate on diatoms (1/day)
phaeo_umax[b]	5.1	maximum grazing rate on *Phaeocystis* (1/day)
z_grz	1.05	coefficient used in zooplankton grazing rate calculation

[a]See *Moore et al.* [2002, 2004] for details. All parameter values for *Phaeocystis* listed here are optimized in section 3.1 and used in the simulation discussed in section 3.2.
[b]Parameter is scaled by the temperature function with Q10 value of 2.0.
[c]Parameter value is scaled by ambient temperature to avoid from over grazing by zooplankton when *Phaeocystis* growth rate decreases at higher temperatures.

were averaged within model grid cells, though observations were often from different years. Furthermore, we compared simulated chlorophyll concentrations and distributions with satellite observations. The surface chlorophyll a concentrations was from the National Aeronautics and Space Administration (NASA) standard OC4v4 algorithm from the SeaWiFS satellite sensor. The best case simulations are defined as simulations in which higher correlations between modeled and observed data are obtained. Data from simulations and observations in each model grid were weighted evenly. Previous observations suggested that *Phaeocystis* generally blooms in coastal regions and has low abundance in most open waters [*Coale et al.*, 2003; *Schoemann et al.*, 2005], which was also a criteria in selecting model parameters.

[22] The BEC model was initially spun up for 800 years to approximately steady state with NCEP/NCAR meteorological reanalysis climatology without *Phaeocystis*. Then the BEC model ran for another 100 years with *Phaeocystis* parameter values identical to the diatom values. This was followed by 25 year sensitivity simulations, which is long enough for drifts in upper ocean ecosystem structure to decline to a negligible level, and short enough to allow a large number of simulations while minimizing drifts in subsurface nutrient fields. In the control simulation, all the parameters for *Phaeocystis* were kept identical to those of diatoms. The *P. antarctica* growth rate reduces progressively at temperatures above 6°C, and the threshold temperature for *P. antarctica* growth is chosen as 10°C, above which *P. antarctica* ceases growing, based on batch culture experiments [*Buma et al.*, 1991].

[23] Photosynthetic parameters of *P. antarctica* derived from literature values were relatively consistent. The average value of photosynthetic efficiency term, alpha (α) for *P. antarctica* colonies from the literature was 0.63 mmol C m^2 (mg Chl W d)$^{-1}$ [*Hong et al.*, 1997; *Matrai et al.*, 1995; *Palmisano et al.*, 1986; *Schoemann et al.*, 2005; *van Hilst and Smith*, 2002] and the maximum of Chl/N ratio of *P. antarctica* in previous research reports was approximately 2.5 mg mmol^{-1} [*van Leeuwe and Stefels*, 1998]. Based on those reported data, we test several groups of photosynthetic parameters around the mean α with the fixed maximum Chl/N ratio from the literature. The maximum of Chl/N ratios of diatoms and small phytoplankton in the model are 4.0 and 2.5 mg mmol^{-1}, respectively. And the α value for diatoms and small phytoplankton in the BEC model are 0.25 and 0.28 mmol C m^2 (mg Chl W d)$^{-1}$, respectively, considerably lower than that observed for *P. antarctica*.

[24] The iron uptake efficiency is one of the proposed key controlling factors for *Phaeocystis*. The cellular iron requirements of *Phaeocystis* vary with irradiance level [*Garcia et al.*, 2009; *Sedwick et al.*, 2007], other environmental conditions, and the estimated half-saturation constants of *P. antarctica* for uptake of iron also vary within a large range. Thus, based on *Coale et al.* [2003], *Sedwick et al.* [2007], and *Garcia et al.* [2009], we test iron half-saturation constants from 0.045 to 0.45 nM Fe. Previous modeling studies have used

more extreme values of 0.01 [*Arrigo et al.*, 2003; *Worthen and Arrigo*, 2004] and 1.5 nM [*Pasquer et al.*, 2005]. The iron half-saturation uptake constant of diatoms is 0.08 nM Fe and for small phytoplankton a value of 0.035 nM Fe is used in the BEC model. The half-saturation constants of *P. antarctica* for uptake of N and P are set identical to those of diatoms due to lack of laboratory and field observational data. N and P are never depleted to growth-limiting concentrations in the *P. antarctica* domain in the model.

[25] In the BEC model, only one grazer group is used to represent both microzooplankton and larger zooplankton, and it feeds on all phytoplankton groups. Previously, phytoplankton groups in the model had distinct sizes and physiological characteristics, and it was assumed that different phytoplankton groups were preyed upon by different zooplankton. Therefore, the grazing expression allowed different grazing rates for different phytoplankton groups and the grazing rates of phytoplankton groups were independent from each other.

[26] However, grazing parameterization became more complex with the presence of *Phaeocystis*. Due to the large size range of *Phaeocystis* colonies, there are many uncertainties of grazing on *P. antarctica*. As reviewed by *Nejstgaard et al.* [2007], many in situ observations and laboratorial incubations showed that *Phaeocystis* colonies can be consumed by copepods, ciliates, and other zooplankton, which can also feed on diatoms. However, some previous observations also suggested that there may be preference of food selection for some zooplankton, which leads to different grazing rates on diatoms and *Phaeocystis*. For example, diatoms satisfied 74% of mesozooplankton carbon demand during *Phaeocystis*-dominated blooms in Belgian coastal waters, while *Phaeocystis* represented 70% of the net primary production [*Rousseau et al.*, 2000]. *Hamm et al.* [1999] reported that the *Phaeocystis* colony was encased in a thin, but very strong, semipermeable skin, which allows inorganic ions pass freely and protects colony cells against grazing and infection by viruses effectively. *Hamm et al.* [1999] suggested low grazing and mortality due to the protection of the colony skin is the key factor responsible for *Phaeocystis* blooms. In our study, the grazing loss of *Phaeocystis* and diatoms are adjusted to be interactional, i.e., the grazing pressure on either *Phaeocystis* or diatoms is influenced by the biomass of both groups (equation (10)). We also tested different maximum grazing rates on *Phaeocystis* and diatoms to examine the relative importance of grazing pressure

$$\text{graze\_phaeo} = \text{phaeo\_umax} * \text{zooC} * \left(\text{phaeoC}^2 / \left((\text{phaeoC} + \text{diatC})^2 + \text{z\_grz}^2\right)\right). \quad (10)$$

The phaeo_umax is the maximum zooplankton grazing rate on *Phaeocystis*. Different values of this parameter are tested and discussed in section 3.1. The zooC term represents zooplankton carbon biomass in mmol/m^3, which is the sum of zooplankton growth by consumption of all phytoplankton groups minus zooplankton losses; z_grz is the grazing coefficient for phytoplankton, which reduces grazing pressure at low phytoplankton biomass; and phaeoC and diatC are the carbon biomass of *Phaeocystis* and diatoms, respectively. A similar formulation was used to compute grazing of diatoms. Some key ecosystem model parameter values are listed in Table 1 (for further details please see *Moore et al.* [2002, 2004]).

3. Results and Discussion

3.1. Simulations of *Phaeocystis*

[27] We compared simulations of *P. antarctica* with different α values with the control experiment, in which the photosynthetic parameter values are set identical to diatoms. Increasing α of *P. antarctica* to the mean laboratory value, 0.63 mmol C m^2 (mg Chl W d)$^{-1}$, improved the logarithmic correlations between simulations and observations of *Phaeocystis* carbon biomass from 0.590 to 0.619; and the logarithmic correlation for diatoms increased from 0.356 to 0.393 (Table 2). This suggested that the higher α value fit the observations better. Although the correlations between simulated chlorophyll distributions and SeaWiFS satellite measured distributions decreased after modifying α value for *P. antarctica*, it was likely because other parameters for *this group* were still identical to diatoms. When we decreased and increased α values ±20% of the observed mean value, there was no significant change in *Phaeocystis* carbon biomass distributions and chlorophyll distributions (Figure 1). Also, the correlations between simulations and observations were similar and the best overall model performance was from the simulation with mean laboratory value. This suggests that simulations of *P. antarctica* are not very sensitive to α values in the range of ±20% of mean laboratory-determined value. We adopted this mean value of 0.63 mmol C m^2 (mg Chl W d)$^{-1}$ for further simulations. In our simulations, to optimize model performance, a higher α value for *P. antarctica* was required, which should allow the *Phaeocystis* group to have an advantage under lower irradiance.

[28] We next experimented on a series of half-saturation constant for uptake of iron (K_{fe}) with the optimized photosynthetic parameters. Compared to the impacts of α on simulation, the BEC model is more sensitive to changes of K_{fe} for *Phaeocystis*. When K_{fe} of *P. antarctica* were 0.045, 0.08, and 0.12 nM, unrealistic carbon biomass distributions resulted, with high biomass in open ocean areas (Figures 2 and 3), which had never been observed in the field. Thus, simulations in which K_{fe} of *Phaeocystis* were in the range of 0.045 ~ 0.12 nM probably overestimated biomass of *P. antarctica*. However, when K_{fe} of *Phaeocystis* was set higher than 0.26 nM, *Phaeocystis* carbon biomass and chlorophyll concentrations were lower than observations, especially in coastal regions (Figures 2 and 3). For example, high carbon biomass of *P. antarctica* and chlorophyll concentrations have been observed in the Crozet-Kerguelen region [*Moore et al.*, 2007; *Poulton et al.*, 2007], where *Phaeocystis* generally contributes to phytoplankton blooms during austral spring and summer. Those simulations with high K_{fe} of *Phaeocystis* probably led to underestimates of *P. antarctica* in the BEC model. When the K_{fe} of *Phaeocystis* was 0.18 and 0.20 nM, better logarithmic correlations between simulated and observed phytoplankton carbon biomass and between simulated chlorophyll distribution and SeaWiFS observation were obtained (Table 3). This suggested that the range of 0.18–0.20 nM for K_{fe} of *Phaeocystis* should be chosen for the BEC model. We also test combinations with K_{fe} of *Phaeocystis* in the range of 0.16 ~ 0.24 nM and α of

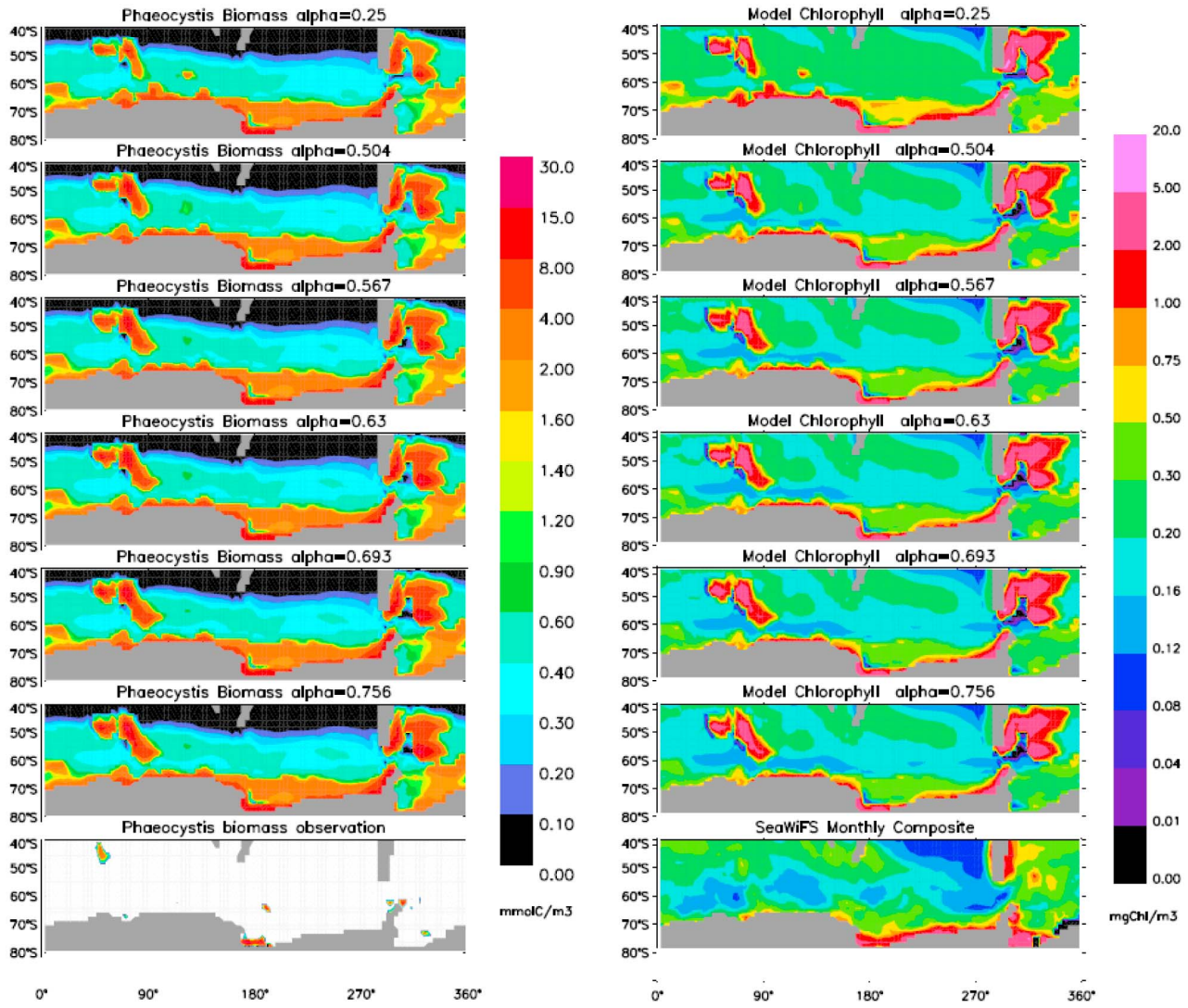

Figure 1. (left) *P. antarctica* surface carbon biomass distributions from simulations with different α values of *Phaeocystis* and observations. (right) Surface chlorophyll *a* concentrations from different simulations and SeaWiFS satellite observations are shown. The value of α in each experiment is listed at the top. In the control run, photosynthetic parameters of *Phaeocystis* were identical to diatoms, the α value of which was 0.25 mmol C m^2 (mg Chl W d)$^{-1}$. Both simulations and observation data were averaged over 4 months (November–February).

Phaeocystis in the range of ±10% of the chosen value in the experiments above. The best simulations were obtained when K_{fe} was 0.18 or 0.20 nM and α was 0.63 mmol C m^2 (mg Chl W d)$^{-1}$. There were no significant differences between simulations with K_{fe} of *Phaeocystis* equal to 0.18 and 0.20 nM. We adopted the value of 0.18 nM for the following simulations. In the BEC model, the K_{fe} of diatoms was 0.08 nM, while the optimized K_{fe} value of *Phaeocystis* was more than twice this value. With such a low iron uptake efficiency, *P. antarctica* in simulations can only bloom in areas, where Fe concentrations are relatively high. This agrees with previous field observations [*Coale et al.*, 2003; *Schoemann et al.*, 2005].

[29] As discussed in section 2.1, a difference in grazing pressure was also proposed to be one of the controlling factors of competition between diatoms and *Phaeocystis*. We

Table 2. Correlation Coefficient *r* Between Modeled and Observed Chlorophyll Concentration and *Phaeocystis* and Diatom Biomass After Log Transformation in Experiments With the Photosynthetic Parameters of *P. antarctica*

	alphaChlphaeo[a]					
	0.25	0.63	0.693	0.756	0.567	0.504
Phaeocystis r	0.590	0.619	0.576	0.621	0.576	0.606
diatom *r*	0.356	0.393	0.334	0.338	0.334	0.401
chlorophyll *r*	0.414	0.373	0.365	0.356	0.376	0.383

[a]Values of α in different experiments, in the unit of mmol C m^2/mg Chl W d. The α is 0.25 mmol C m^2/mg Chl W d in the control run, in which parameters for diatoms and *Phaeocystis* are set the same. The value of 0.63 mmol C m^2/mg ChlWd is the mean value calculated based on data from *Palmisano et al.* [1986], *Matrai et al.* [1995], *Hong et al.* [1997], and *van Hilst and Smith* [2002]. We increased and decreased 10% and 20% of α for *Phaeocystis*.

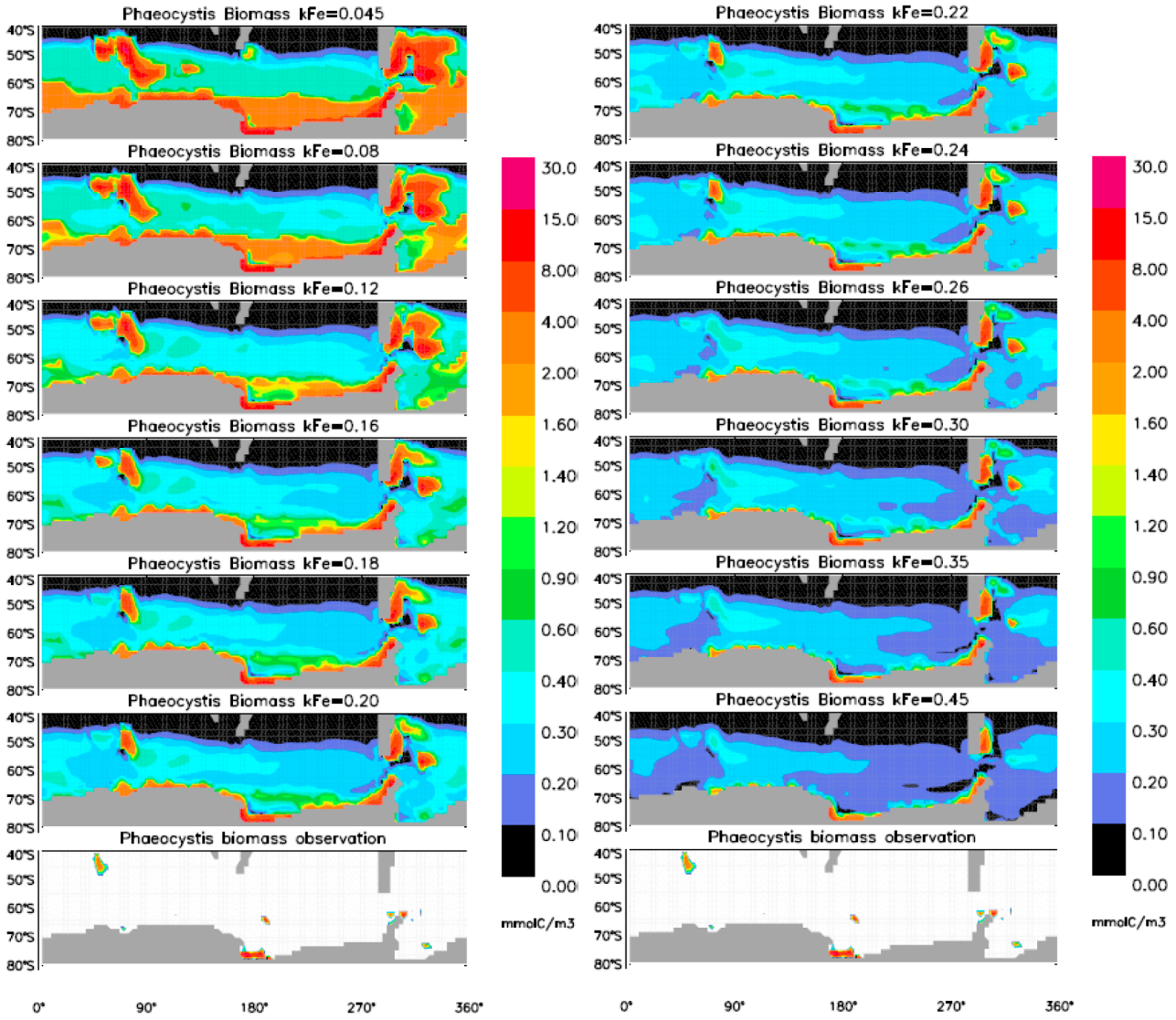

Figure 2. *P. antarctica* surface carbon biomass distributions from simulations with varying half-saturation constants for iron uptake (K_{fe}) values for *Phaeocystis* are compared to observed biomass. Both simulation and observation data were averaged over summer months.

changed relative grazing rates on diatoms and *Phaeocystis* in simulations with the optimized *Phaeocystis* K_{fe} and α values. As shown in Table 4, when grazing rates on diatoms and *Phaeocystis* increased by 5% or 10% compared to the original value, the logarithmic correlations between simulated *Phaeocystis* carbon biomass and observation data and the chlorophyll correlations remained similar (about 0.65 and 0.42, respectively). However, this logarithmic correlation of diatoms in the simulations dropped when maximum grazing rate on only one group was increased 5%. Lowering grazing pressure on *Phaeocystis* or diatoms by similar amounts did not improve simulation results either. Larger changes in grazing rate (20%) resulted in even lower correlations with the observations (not shown). Best results were obtained when *Phaeocystis* and diatoms experienced similar grazing pressure. Thus, to better match observations of both phytoplankton groups, the grazing parameters of diatoms and *Phaeocystis* in the BEC model were set the same. Although, some preference of food selection by zooplankton has been observed, our simulations cannot identify the significance of different grazing pressure in controlling phytoplankton competition, at least when the zooplankton group is highly simplified, as in the BEC model.

[30] In our simulations, the growth of *Phaeocystis* was limited by high temperature over about 25% of the Southern Ocean over the annual cycle (Figure 4). This is because *P. antarctica* growth is suppressed in the BEC model when sea surface temperatures are greater than 6°C and growth ceases above 10°C. Light was rarely the most limiting factor of growth for *P. antarctica*, less than 1% of ocean area. However, growth of *P. antarctica* was limited by iron availability over approximately 73% of the Southern Ocean. Iron was even insufficient for *Phaeocystis* growth in the Crozet-Kerguelen region, where the other phytoplankton groups were not iron limited (Figure 4).

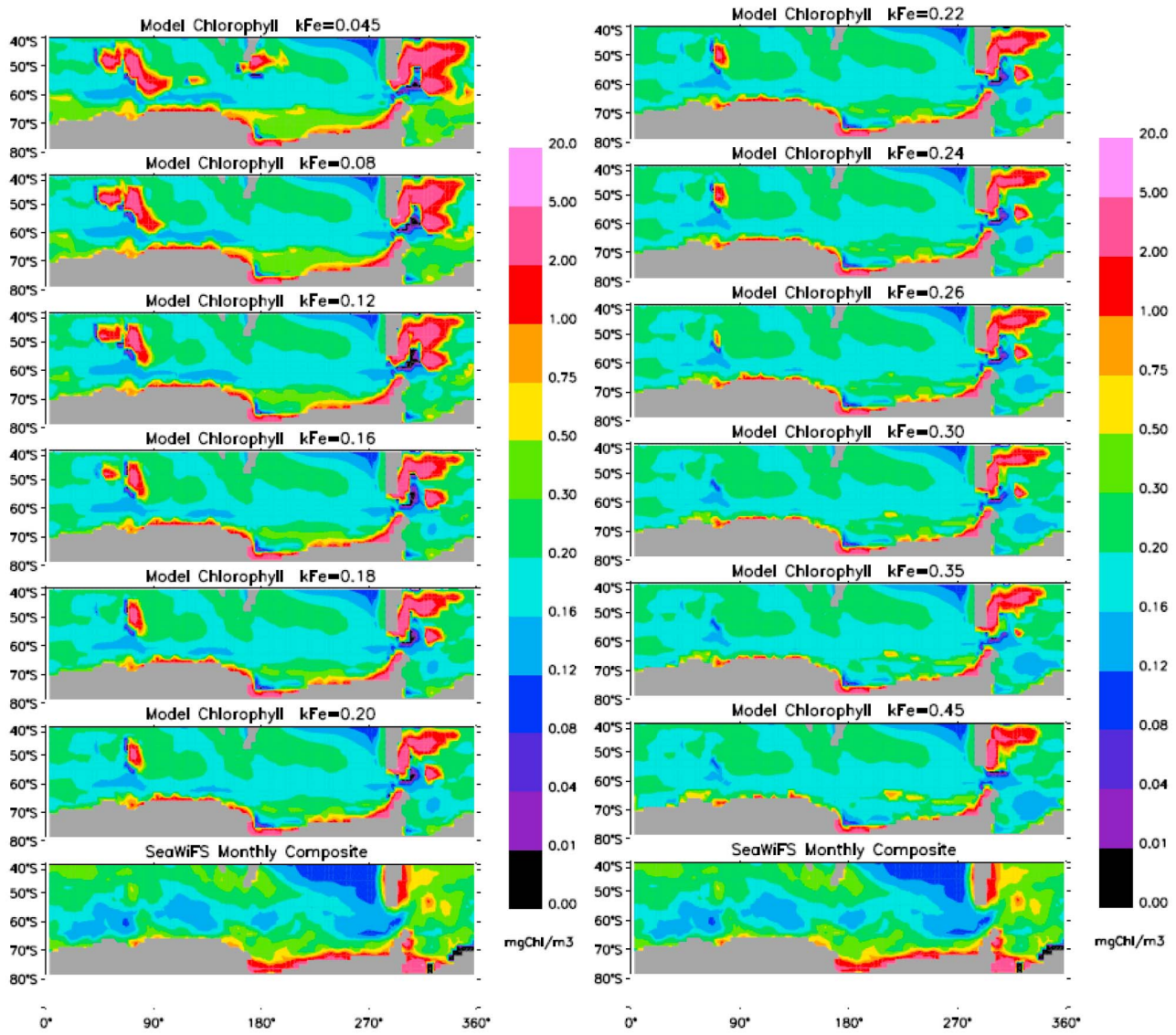

Figure 3. Surface chlorophyll *a* concentrations from different simulations and SeaWiFS satellite observations. Description of simulations is as in Figure 2.

[31] For the growth of diatoms, light was the most limiting factor over about 8.7% of the Southern Ocean, especially in the Ross Sea and the Weddell Sea, the southernmost regions, where iron concentrations tend to be higher. Iron typically limited the growth of diatoms in the open ocean. The growth of diatoms was also limited by N and Si in 3.5% and 5.8% of the total area, respectively, near the northern boundary of our study domain. These areas were closer to Australia and South America, where iron concentrations were high enough to support diatom growth. *P. antarctica* cannot compete in these areas as a result of warm temperatures. The distributions of most limiting factors for growth indicated that the interplay of light and iron availability largely controlled the competition between diatoms and

Table 3. Displayed are the Correlation Coefficients *r* Between Modeled and Observed Data in Experiments of Iron Uptake Efficiency by *P. antarctica*

	K_{fe}[a]											
	0.045	0.08	0.12	0.16	0.18	0.2	0.22	0.24	0.26	0.3	0.35	0.45
Phaeocystis r	0.595	0.619	0.612	0.582	0.646	0.632	0.589	0.588	0.586	0.582	0.581	0.571
diatom *r*	0.083	0.393	0.403	0.278	0.291	0.293	0.293	0.291	0.164	0.22	0.207	0.203
chlorophyll *r*	0.324	0.373	0.385	0.402	0.416	0.418	0.411	0.418	0.414	0.399	0.41	0.386

[a]Half-saturation constant value for *Phaeocystis* iron uptake (nM).

Table 4. Displayed are the Correlation Coefficients *r* Between Modeled and Observed Data in Experiments of Varying Grazing Pressure on *P. antarctica* and Diatoms

	*Phaeocystis*_umax, diatom_umax[a]						
	5.1, 5.1	5.1, +5%	5.1, +10%	5.1, −5%	−5%, 5.1	+5%, 5.1	+10%, 5.1
Phaeocystis *r*	0.646	0.651	0.653	0.580	0.548	0.649	0.649
diatom *r*	0.291	0.177	0.227	0.271	0.325	0.172	0.219
chlorophyll *r*	0.416	0.420	0.428	0.399	0.388	0.415	0.418

[a]*Phaeocystis*_umax and diatom_umax are the maximum zooplankton growth rate (1/day) on *Phaeocystis* and diatoms, respectively, which indicate the relative grazing pressure on phytoplankton groups. Here percents indicate an increase/decrease of percentage of original value.

P. antarctica in the southernmost regions, such as the Ross Sea and the Weddell Sea. However, iron availability alone mainly controls the distributions and biomass of diatoms and *P. antarctica* in the open ocean. For small phytoplankton, some top-down grazing control of biomass was apparent, which appears as replete or light limited in Figure 4.

[32] The carbon biomass distributions of *P. antarctica* and diatoms in Figure 5 also indicated the major controlling factor in different regions. Carbon biomass of *Phaeocystis* and diatoms around the Crozet-Kerguelen region and south of South America both increased when only α of *Phaeocystis* was increased to the optimal value, when other parameters of *Phaeocystis* were kept identical to diatoms (Figure 5). However, the biomass of *Phaeocystis* remained similar in the Ross Sea and Weddell Sea, while biomass of diatoms was lower in those two regions. This suggested that light dependence of the phytoplankton groups was very important for regulating phytoplankton competition in the Ross Sea and the Weddell Sea. Since *Phaeocystis* had a higher α value, it had a competitive advantage, especially in spring and early summer when irradiance levels were lower and mixed layer depths were deeper.

[33] In our simulations, when we only changed K_{fe} of *Phaeocystis* to the optimized value (0.18 nM) and other parameters kept identical to diatoms, the distributions of *Phaeocystis* and diatoms changed significantly. Both *Phaeocystis* and diatom biomass decreased in the Ross Sea, the Weddell Sea, south of the South America and the Crozet-Kerguelen regions. However, the proportions of primary production by *Phaeocystis* and diatoms changed differently in the open ocean. *Phaeocystis* biomass decreased significantly in the open ocean compared to that in simulations in which parameters of *Phaeocystis* are identical to diatoms, while diatoms biomass in the open ocean remained at similar levels. This suggested that different iron uptake efficiencies significantly influenced the competition between *Phaeocystis* and diatoms, especially in the open ocean where the iron concentrations were relatively low.

[34] In our simulations, changing grazing rates influenced only total carbon biomass and phytoplankton production. Furthermore, changing grazing pressure the same magnitude for *Phaeocystis* and diatoms showed similar phytoplankton and chlorophyll distributions (Figure 5). The competition between diatoms and *P. antarctica* in the BEC model was not particularly sensitive to changes in grazing rates. This agrees with *Tagliabue and Arrigo* [2003], which suggested that high *Phaeocystis* biomass and low zooplankton abundance observed in the Ross Sea polynya can be explained by the zooplankton-phytoplankton decoupling, instead of grazing preference. However, the biomass of these two phytoplankton groups are related to each other through the grazing loss term in the BEC model, and the treatment of zooplankton in the model is relatively simple. We cannot draw firm conclusions about the role of grazing differences in the competition between diatoms and *P. antarctica*. Further studies of the role of grazing in this competition are warranted.

3.2. Ecosystem Simulations With the BEC Model

[35] Our best case BEC simulation, with the mean laboratory α value and a K_{fe} of 0.18 nM for *P. antarctica*, was able to reasonably reproduce patterns of primary and export production, biogenic silica production, chlorophyll, and macronutrients concentrations in field observed data. The

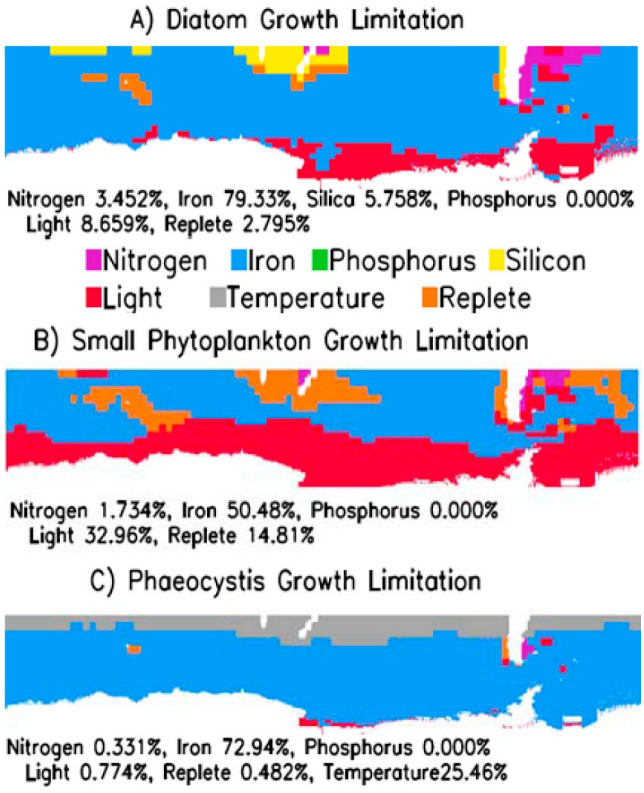

Figure 4. Factors that are most limiting the surface growth rates of (a) diatoms, (b) small phytoplankton, and (c) *P. antarctica* in the Southern Ocean from the best case simulation over the annual timescale.

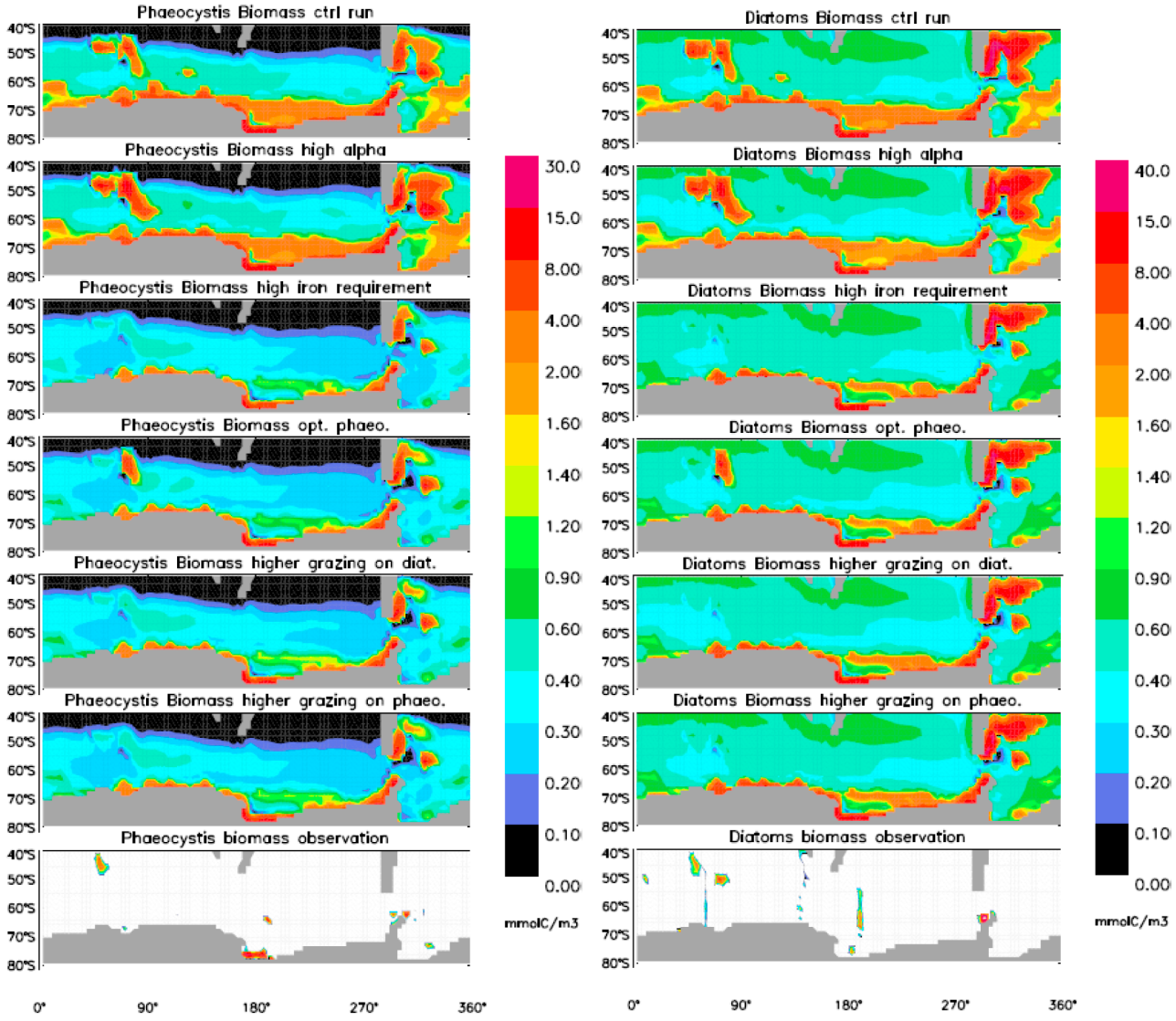

Figure 5. *P. antarctica* and diatoms surface carbon biomass distributions from simulations with different parameters of *Phaeocystis* and diatoms. The notations are as follow: ctrl run, all parameters of *Phaeocystis* are identical to diatoms; high alpha, *Phaeocystis* group has higher α value, 0.63 mmol C m^2 (mg Chl W d)$^{-1}$; high iron requirement, K_{fe} of *Phaeocystis* is 0.18 nM; opt. phaeo, *Phaeocystis* group has both optimized α and K_{fe}; higher grazing on diat., grazing pressure on diatoms increases 5%; higher grazing on phaeo, grazing pressure on *Phaeocystis* increases 5%. The model output was averaged over summer months.

logarithmic correlations between simulated and observed *P. antarctica* and diatom carbon biomass are 0.646 and 0.291, respectively (Figure 6). Simulations of *P. antarctica* match well most of the field data in different regions. However, model simulations tended to underestimate *P. antarctica* biomass around Crozet-Kerguelen region. This is in part because the circulation and nutrient distribution field were not well captured in this region, due to the coarse resolution of the ocean circulation model, particularly near the Crozet Plateau. This region is also near the boundary where the simulated *Phaeocystis* growth is reduced at higher temperatures. There are only limited studies of the effects of temperature on growth. The model-data mismatch in Figure 6 is likely due to a number of additional factors not accounted for in the model simulations, such as interannual variations in forcings (wind, sea ice cover, temperature, and dust deposition) and processes not included in the model, such as transport of iron within sea ice [*Lancelot et al.*, 2009].

[36] *P. antarctica* carbon biomass was generally lower than diatom carbon biomass, especially in the open ocean. However, *P. antarctica* could have a similar contribution to primary production as diatoms in coastal, nutrient-rich waters (Figure 7). Overall, *Phaeocystis* generally formed blooms where iron concentrations were high in our simulations due to the lower iron uptake capacity for growth. Also, *Phaeocystis* made up a higher percentage of total phytoplankton biomass in spring and early summer when irradiance levels were lower. During austral spring and summer, *P. antarctica*

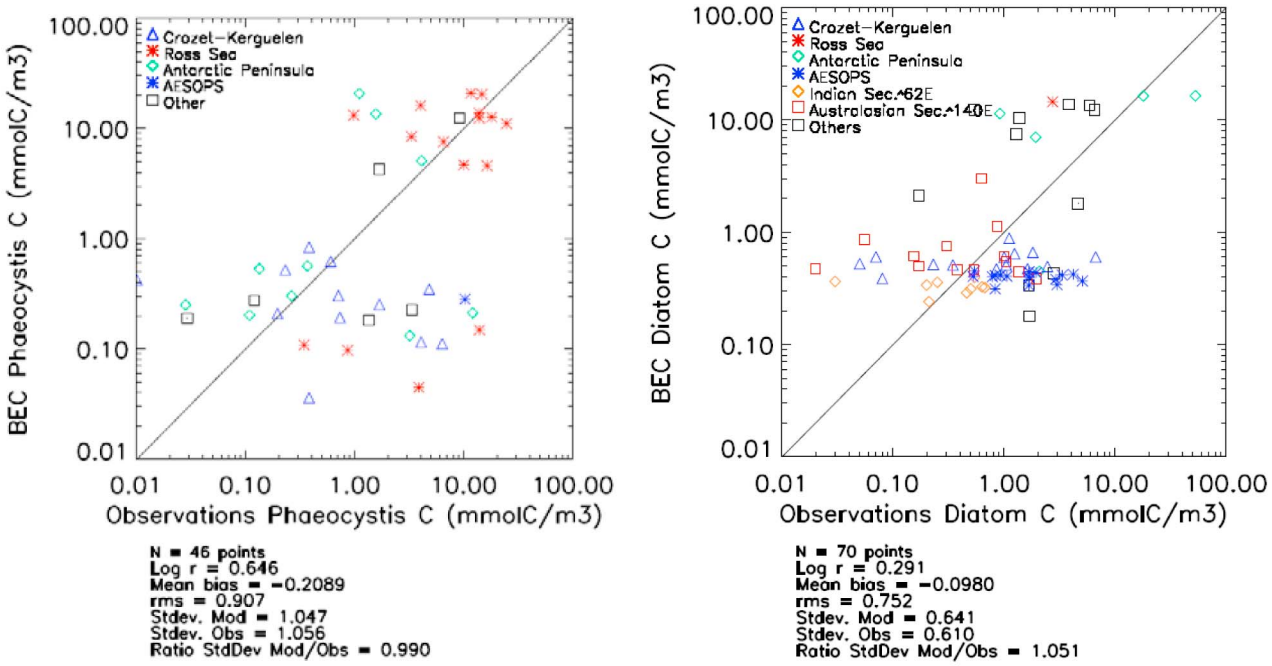

Figure 6. Comparisons of simulated and observed (left) *P. antarctica* carbon biomass and (right) diatoms carbon biomass. Data were from the Crozet-Kerguelen region (blue triangles), the Ross Sea (red asterisks), Antarctic Peninsula (green diamonds), the AESOPS study area (blue asterisks), Indian sector (orange diamonds), Australasian sector (orange squares), and other regions in the Southern Ocean (black squares). Model outputs are from the simulation with optimized parameters.

contributed to 10–30% primary production, less than small phytoplankton and diatoms. However, 40–50% of total production in Crozet-Kerguelen region, the Ross Sea and the Weddell Sea in early spring (November) were contributed by *P. antarctica* (Figure 7). The development of blooms of *P. antarctica* was earlier than that of diatoms, however, the peak biomass of *P. antarctica* and diatoms were both in January. The blooms of all phytoplankton groups vanished quickly in February due to the depletion of iron.

[37] We evaluate the model performance in our best case simulation by comparing various biogeochemical and physical variables with the corresponding observations using Taylor diagrams (Figure 8). Taylor diagrams indicate the correlation between model and observations (along curved axis) and the normalized variance (model standard deviation divided by the observational standard deviation, on the x and *y* axis [*Taylor*, 2001]). This is a compact way to present a quantitative assessment of model performance. The model does a very good job of reproducing the observed fields for nitrate, phosphate, and dissolved silicon in the Southern Ocean, with correlation coefficients > 0.85 and variability somewhat underestimated (Figure 8, left). The correlation for iron is much lower, but the observational database for iron is very small (~900 Southern Ocean measurements) and likely does not accurately capture the large-scale distribution. There are hundreds of thousands of observations for each of the macronutrients in the WOA database. The correlation coefficients for chlorophyll, salinity, and mixed layer depths range between 0.44 and 0.63 (Figure 8, right). The salinity mismatches are largely due to the use here of prescribed satellite-based sea ice cover, and would likely be significantly improved with a coupled sea ice model. For both the macronutrients and the chlorophyll the performance of the model here in the Southern Ocean is better than previous results at the global scale [*Doney et al.*, 2009]. The model does an excellent job of reproducing the observed temperature fields in the Southern Ocean, with a correlation of 0.94 and a relative variability close to 1.0 for the model layer centered on a depth of 149 m. Sea surface temperatures are strongly pushed toward the observations by the prescribed atmospheric forcing. The subsurface temperature used here is a function of those atmospheric forcings and the circulation and mixing processes in the model.

[38] Spatial distributions of sea surface temperature, mixed layer depth, surface PAR, and iron concentrations for summer season (November–February) in our best case simulation are shown in Figure 9. The mixed layer depths are still deep in November, especially between 50°S~70°S, then the mixed layer depths decreased sharply in December. The surface PAR also peaks in December, concurrently with significant increases in phytoplankton biomass. The surface iron concentrations are highest in November and declined to a much lower level after the growing season (Figure 9).

[39] We also compared simulations with and without *P. antarctica* in the BEC model. With other parameters and conditions the same, adding *P. antarctica* in the BEC model caused a slight decrease of total primary production in the Southern Ocean from 8.69 to 8.24 Gt C. Total sinking particulate organic carbon (POC) flux at 103 m depth remained similar with the contribution of *P. antarctica*. In simulations without *P. antarctica*, approximate 47.8% of primary production was from small phytoplankton group in the BEC

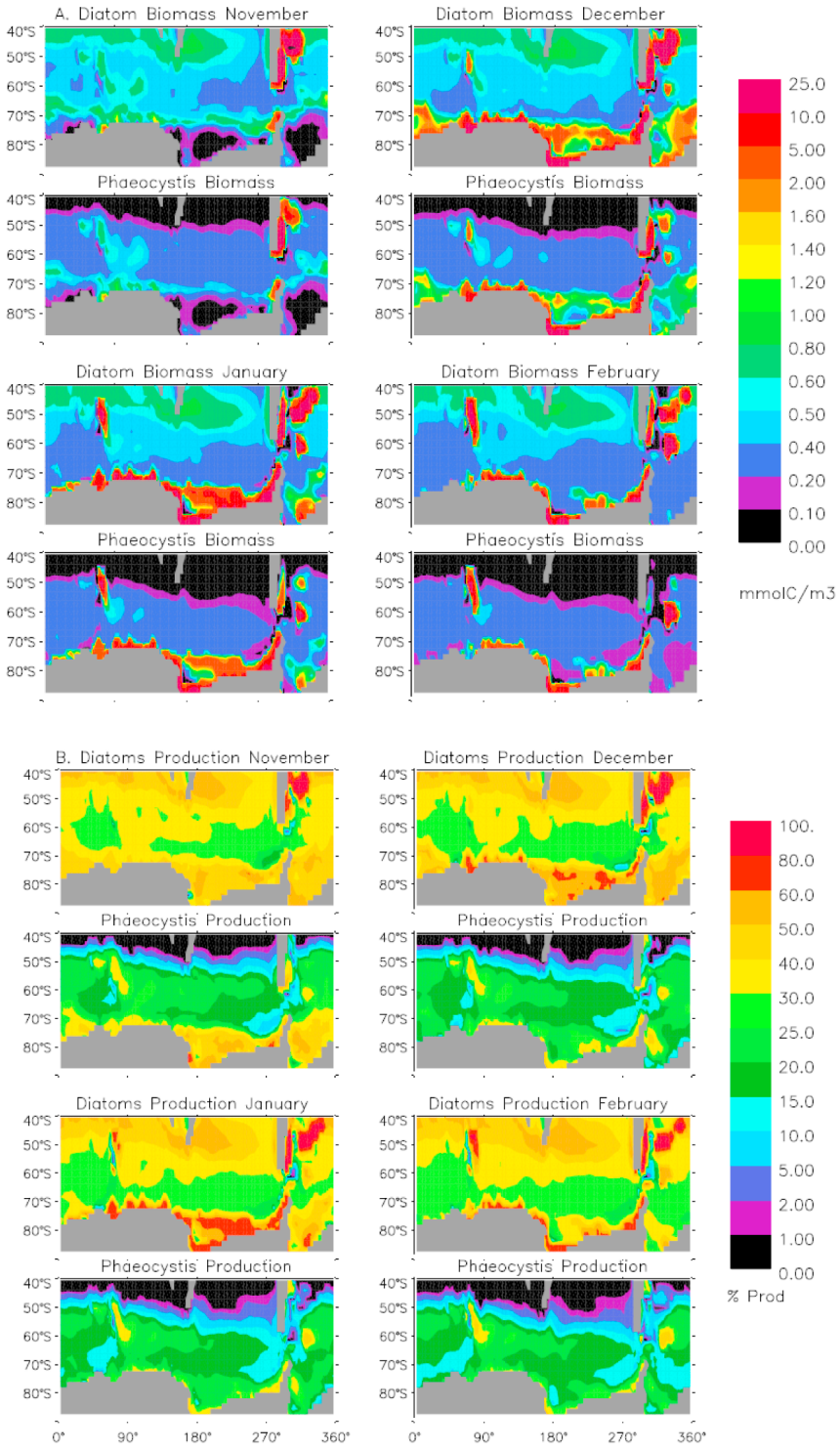

Figure 7. (a) Carbon biomass distributions and (bottom) the percentage of primary production by diatoms, small phytoplankton, and *P. antarctica* in the Southern Ocean over summer months (November–February) in our best case simulation.

model, and 52.2% was from diatoms. After we incorporated *P. antarctica* in the model, primary production attributed to small phytoplankton decreased 4.1% and primary production from diatoms decreased 8.9%, and *P. antarctica* accounted for about 13.0% of primary production. In simulations with *P. antarctica*, diatoms contributed to 59.2% of sinking POC export and *P. antarctica* contributed to 18.6% of sinking POC export. With *P. antarctica* in the BEC model, calcification and biogenic Si production decreased about 21 and 7%, respectively. The contribution of *P. antarctica* to

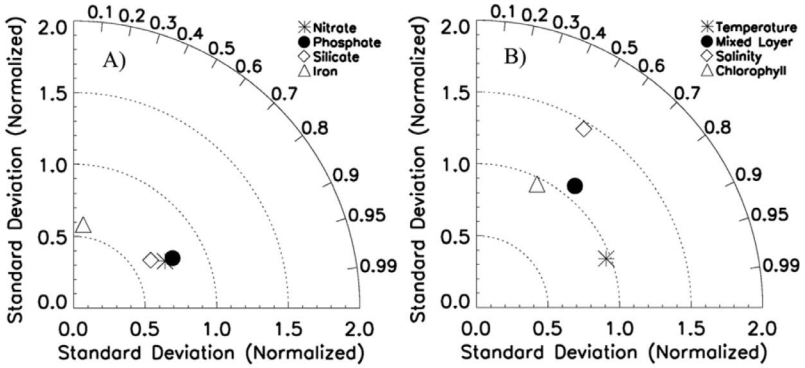

Figure 8. Taylor diagrams quantifying the model performance in reproducing observed biogeochemical and physical fields [*Taylor*, 2001]. Temperature, salinity, and macronutrient concentrations are from the World Ocean Atlas 2005 [*Antonov et al.*, 2006; *Garcia et al.*, 2006; *Locarnini et al.*, 2006]. Temperature is from the model layer centered at 149 m depth, and the nutrients and salinity are surface values. Iron concentrations over the upper 504 m are compared with observations from the database compiled by *Moore and Braucher* [2008]. Monthly mixed layer depths are compared with the observational estimates from *de Boyer Montégut et al.* [2004].

primary production was much smaller than diatoms and small phytoplankton over the whole Southern Ocean. However, much of the *P. antarctica* production was from areas along coasts and other nutrient-rich regions, with their contribution accounting for ~22.7% of primary production, and ~30.0% of the sinking POC export at high latitudes (>60°S), thus the impact of *P. antarctica* on Southern Ocean biogeochemistry was significant.

4. Conclusions

[40] *Phaeocystis* has been included in biogeochemical models in recent years to understand its ecological roles and the contribution of *Phaeocystis* to the biological carbon pump [*Arrigo et al.*, 2003; *Gypens et al.*, 2004; *Lancelot et al.*, 2000; *Pasquer et al.*, 2005]. Incorporating *Phaeocystis* in the BEC model is an approach to study the role of *P. antarctica* on biogeochemical cycles, the carbon budget, and the competition between *P. antarctica* and diatoms in the Southern Ocean.

[41] In general, the modified BEC model can simulate the basic distributional patterns of *Phaeocystis*, which are consistent with previous field observations. By comparing simulations with and without *P. antarctica*, we found that simulations without *P. antarctica* likely overestimated contributions of diatoms to primary production and sinking POC export. Although, *P. antarctica* contribution to primary production was smaller than diatoms and small phytoplankton, 18.6% of total sinking POC export was attributed to *P. antarctica* (30% of POC export for latitudes >60°S). *P. antarctica* was especially important in the marine ecosystem in some coastal areas, such as the Ross Sea and the Weddell Sea.

[42] Some previous studies suggested that the distributions of diatoms and *Phaeocystis* are determined by the water column structure and its vertical stability. Diatoms bloomed in highly stratified, iron-enriched, ice edge or coastal water columns, while *Phaeocystis* was better adapted to a deep mixing and weakly stratified waters within the Ross Sea [*Arrigo et al.*, 1999, 2003; *Goffart et al.*, 2000; *Jochem et al.*, 1995; *Weber and El-Sayed*, 1987]. On the other hand, other studies indicated no significant mixed layer depth difference between the dominances of diatoms and *P. antarctica* [*Smith and Asper*, 2001], and no significant differences in photosynthetic parameters between diatoms and *Phaeocystis* in the Ross Sea polynya [*van Hilst and Smith*, 2002]. *Feng et al.* [2010] observed an increased relative abundance of *P. antarctica* under high irradiance. Iron addition experiments suggested that the abundance of iron may be an important factor controlling the distributions of *P. antarctica* and diatoms [*Coale et al.*, 2003; *Moore et al.*, 2007]. However, *Feng et al.* [2010] suggested *P. antarctica* was not more iron stressed than diatoms and that the influences of light and iron on competition between diatoms and *P. antarctica* strongly interacted. *Sedwick et al.* [2007] also suggested the requirement of iron for phytoplankton growth decreases along with the increase of light, so that the impact of low iron availability during spring would be mitigated by the increased irradiance. The BEC model does not currently include these light-iron interactions. Thus, the iron limitation of the growth of *Phaeocystis* from spring may be overestimated in our results, particularly in regions with shallower mixed layers.

[43] Our simulations with the modified BEC model indicated that the interplay of light and iron availability was regulating *P. antarctica* growth, and influencing the competition between diatoms and *P. antarctica* in the southernmost areas of the Southern Ocean, including the Ross Sea and the Weddell Sea. However, iron uptake dynamics was the major controlling factor in the open ocean. Grazing pressure regulated the total phytoplankton biomass, however, differences in grazing pressure did not lead to big changes in the competition between diatoms and *P. antarctica* in our simulations. However, current understanding of grazing on *Phaeocystis* and its interaction with grazing on diatoms are still poorly understood. Also, only *Phaeocystis* colonies are included in the BEC model, which is not able to comprehensively represent the grazing loss of both colonies

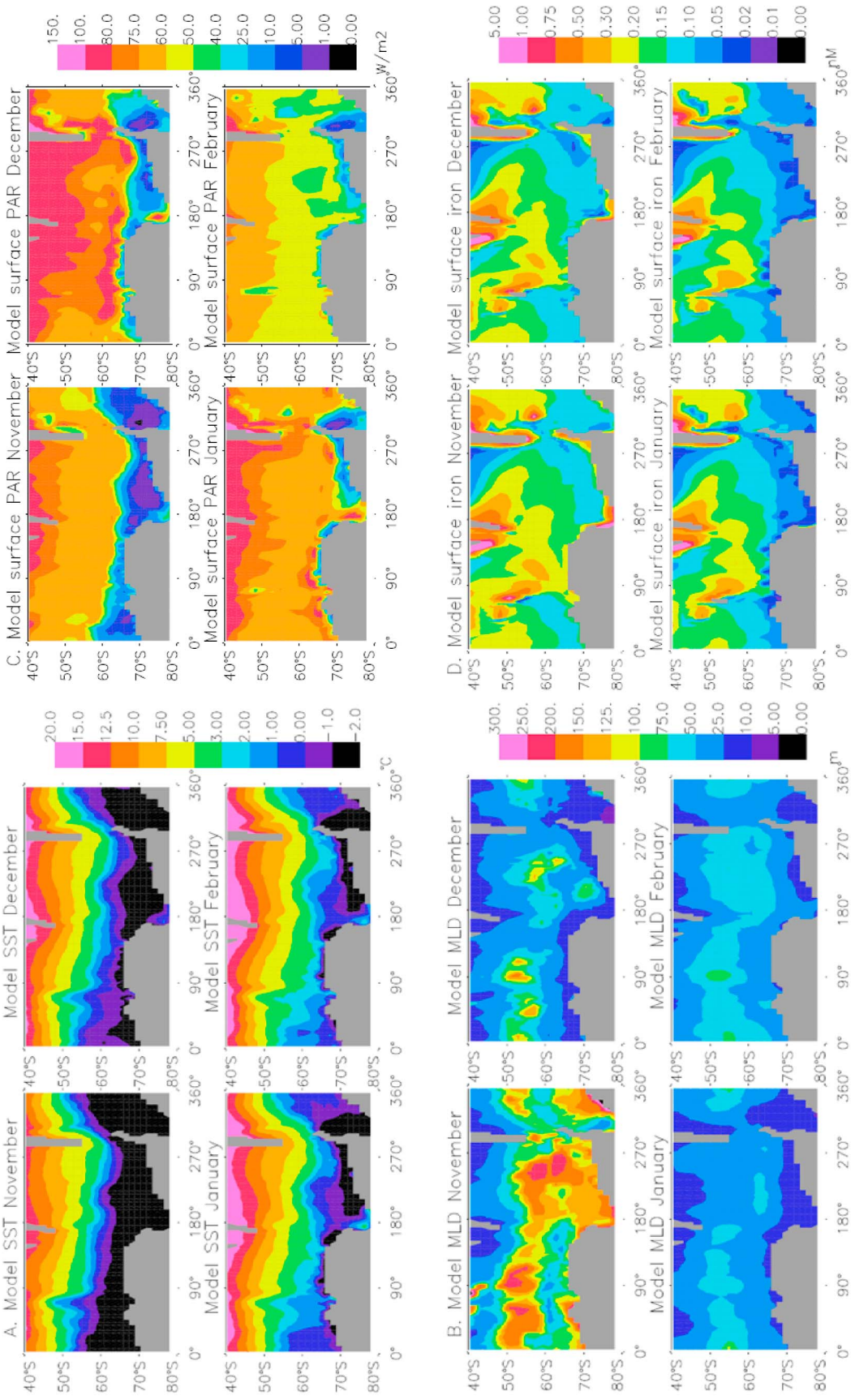

Figure 9. Horizontal distributions of (a) sea surface temperature, (b) mixed layer depth, (c) surface PAR, and (d) surface iron concentration for the summer season (November–February) in our best case simulation.

and solitary cells. Further studies are needed to improve our understanding of the influence of grazers on Southern Ocean phytoplankton community structure.

[44] All model parameters were chosen to best match observational data, including phytoplankton carbon biomass, and variables related to the physical and chemical environment. However, there is still only limited information on nutrient uptake, stoichiometry, and other model parameter values for *Phaeocystis*. The understanding of grazing and other loss processes is also limited. Further laboratory and field work could better constrain the model parameter values. Additional phytoplankton group-specific carbon biomass estimates from the field would also be extremely valuable to constrain modeling efforts. There is also hope for satellite-based approaches for estimating community structure in the future [*Alvain et al.*, 2008]. Though the mixed layer field has been largely improved in current coupled CCSM/BEC model, some bias remained, which may result in errors in light field and nutrient distributions in the model. There are still uncertainties and bias in simulated carbon biomass and chlorophyll distribution induced by bias in physical mixing. It is necessary to further improve ocean physical modeling to better simulate mixed layer depths.

[45] Some recent modeling papers discussed the effects of interactions between iron and light [e.g., *Mongin et al.*, 2007] and some experimental reports related nutrient colimitation on phytoplankton growth [*Bertrand et al.*, 2007; *Saito and Goepfert*, 2008]. These iron-light interactions are not currently included in our model, but could be incorporated in the future. The model settings of α is simplified, with no changes under different light regimes or position in the euphotic zone. The BEC model currently has five phytoplankton functional groups, which are considered most important to represent the oceanic phytoplankton community and biogeochemical cycling. However, there are other important functional groups, like phytoflagellates and the solitary form of *Phaeocystis* in the Southern Ocean, which could be added explicitly in future model simulations.

[46] **Acknowledgments.** We thank all the researchers, technicians, and students who conducted the *Phaeocystis* and diatom laboratory and field studies that made this work possible. We thank David Hutchins and Peter Sedwick for making preprints of papers available. We also thank Véronique Schoemann for sharing the *Phaeocystis* carbon biomass database from their review paper [*Schoemann et al.*, 2005]. In addition, we thank Kevin Arrigo, Giacomo DiTullio, David Hutchins, Peter Sedwick, and Walker Smith Jr. for helpful conversations and suggestions. Helpful comments by anonymous reviewers and the editors significantly improved this paper. This work was supported by funding from NASA grants NNG05GR25G and NNX08AB76G to J. K. Moore. Computations were supported by the Earth System Modeling Facility at UCI (NSF ATM- O321380).

References

Alvain, S., C. Moulin, Y. Dandonneau, and H. Loisel (2008), Seasonal distribution and succession of dominant phytoplankton groups in the global ocean: A satellite view, *Global Biogeochem. Cycles*, *22*, GB3001, doi:10.1029/2007GB003154.

Antonov, J. I., R. A. Locarnini, T. P. Boyer, A. V. Mishonov, and H. E. Garcia (2006), *World Ocean Atlas 2005*, vol. 2, *Salinity*, *NOAA Atlas NESDIS*, vol. 62, edited by S. Levitus, 182 pp., NOAA, Silver Spring, Md.

Armstrong, R. A., C. Lee, J. I. Hedges, S. Honjo, and S. G. Wakeham (2002), A new, mechanistic model for organic carbon fluxes in the ocean based on the quantitative association of POC with ballast minerals, *Deep Sea Res. Part II*, *49*(1–3), 219–236, doi:10.1016/s0967-0645(01)00101-1.

Arrigo, K. R., and G. L. Van Dijken (2007), Interannual variation in air-sea CO_2 flux in the Ross Sea, Antarctica: A model analysis, *J. Geophys. Res.*, *112*, C03020, doi:10.1029/2006JC003492.

Arrigo, K. R., D. H. Robinson, D. L. Worthen, R. B. Dunbar, G. R. DiTullio, M. VanWoert, and M. P. Lizotte (1999), Phytoplankton community structure and the drawdown of nutrients and CO_2 in the Southern Ocean, *Science*, *283*(5400), 365–367, doi:10.1126/science.283.5400.365.

Arrigo, K. R., D. L. Worthen, and D. H. Robinson (2003), A coupled ocean-ecosystem model of the Ross Sea: 2. Iron regulation of phytoplankton taxonomic variability and primary production, *J. Geophys. Res.*, *108*(C7), 3231, doi:10.1029/2001JC000856.

Asper, V. L., and W. O. Smith Jr. (1999), Particle fluxes during austral spring and summer in the southern Ross Sea, Antarctica, *J. Geophys. Res.*, *104*(C3), 5345–5359, doi:10.1029/1998JC900067.

Bertrand, E. M., M. A. Saito, J. M. Rose, C. R. Riesselman, M. C. Lohan, A. E. Noble, P. A. Lee, and G. R. DiTullio (2007), Vitamin B12 and iron colimitation of phytoplankton growth in the Ross Sea, *Limnol. Oceanogr.*, *52*(3), 1079–1093, doi:10.4319/lo.2007.52.3.1079.

Buma, A. G. J., N. Bano, M. J. W. Veldhuis, and G. W. Kraay (1991), Comparison of the pigmentation of two strains of the prymnesiophyte *Phaeocystis* sp, *Neth. J. Sea Res.*, *27*(2), 173–182, doi:10.1016/0077-7579(91)90010-X.

Coale, K. H., X. Wang, S. J. Tanner, and K. S. Johnson (2003), Phytoplankton growth and biological response to iron and zinc addition in the Ross Sea and Antarctic Circumpolar Current along 170°W, *Deep Sea Res. Part II*, *50*(3–4), 635–653, doi:10.1016/S0967-0645(02)00588-X.

Collins, W. D., et al. (2006), The Community Climate System Model Version 3(CCSM3), *J. Clim.*, *19*(11), 2122–2143, doi:10.1175/JCLI3761.1.

Conkright, M. E., R. A. Locarnini, H. E. Garcia, T. D. O'Brien, T. P. Boyer, C. Stephens, and J. J. Antonov (2002), *World Ocean Atlas 2001: Objective Analyses, Data Statistics, and Figures* [CDROM], *Intern. Rep. 17*, 17 pp., Natl. Oceanogr. Data Cent., Silver Spring, Md.

de Baar, H. J. W., et al. (2005), Synthesis of iron fertilization experiments: From the Iron Age in the Age of Enlightenment, *J. Geophys. Res.*, *110*, C09S16, doi:10.1029/2004JC002601.

de Boyer Montégut, C., G. Madec, A. S. Fischer, A. Lazar, and D. Iudicone (2004), Mixed layer depth over the global ocean: An examination of profile data and a profile-based climatology, *J. Geophys. Res.*, *109*, C12003, doi:10.1029/2004JC002378.

Dennett, M. R., S. Mathot, D. A. Caron, W. O. Smith, and D. J. Lonsdale (2001), Abundance and distribution of phototrophic and heterotrophic nano- and microplankton in the southern Ross Sea, *Deep Sea Res. Part II*, *48*(19–20), 4019–4037, doi:10.1016/S0967-0645(01)00079-0.

DiTullio, G. R., J. M. Grebmeier, K. R. Arrigo, M. P. Lizotte, D. H. Robinson, A. Leventer, J. P. Barry, M. L. VanWoert, and R. B. Dunbar (2000), Rapid and early export of *Phaeocystis antarctica* blooms in the Ross Sea, Antarctica, *Nature*, *404*(6778), 595–598, doi:10.1038/35007061.

Doney, S. C., et al. (2004), Evaluating global ocean carbon models: The importance of realistic physics, *Global Biogeochem. Cycles*, *18*, GB3017, doi:10.1029/2003GB002150.

Doney, S. C., I. Lima, J. K. Moore, K. Lindsay, M. J. Behrenfeld, T. K. Westberry, N. Mahowald, D. M. Glover, and T. Takahashi (2009), Skill metrics for confronting global upper ocean ecosystem-biogeochemistry models against field and remote sensing data, *J. Mar. Syst.*, *76*(1–2), 95–112, doi:10.1016/j.jmarsys.2008.05.015.

Feng, Y., et al. (2010), Interactive effects of iron, irradiance and CO_2 on Ross Sea phytoplankton, *Deep Sea Res. Part I*, *57*(3), 368–383, doi:10.1016/j.dsr.2009.10.013.

Fryxell, G. A., and G. A. Kendrick (1988), Austral spring microalgae across the Weddell Sea ice edge: Spatial relationships found along a northward transect during AMERIEZ 83, *Deep Sea Res. Part A*, *35*(1), 1–20, doi:10.1016/0198-0149(88)90054-4.

Garcia, H. E., R. A. Locarnini, T. P. Boyer, and J. I. Antonov (2006), *World Ocean Atlas 2005*, vol. 4, *Nutrients (Phosphate, Nitrate, Silicate)*, *NOAA Atlas NESDIS*, vol. 64, 396 pp., edited by S. Levitus, NOAA, Silver Spring, Md.

Garcia, N. S., P. N. Sedwick, and G. R. DiTullio (2009), Influence of irradiance and iron on the growth of colonial *Phaeocystis antarctica*: Implications for seasonal bloom dynamics in the Ross Sea, Antarctica, *Aquat. Microb. Ecol.*, *57*(2), 203–220, doi:10.3354/ame01334.

Geider, R. J., H. L. MacIntyre, and T. M. Kana (1998), A dynamic regulatory model of phytoplanktonic acclimation to light, nutrients, and temperature, *Limnol. Oceanogr.*, *43*(4), 679–694, doi:10.4319/lo.1998.43.4.0679.

Goffart, A., G. Catalano, and J. H. Hecq (2000), Factors controlling the distribution of diatoms and *Phaeocystis* in the Ross Sea, *J. Mar. Syst.*, *27*(1–3), 161–175, doi:10.1016/S0924-7963(00)00065-8.

Gruber, N., et al. (2009), Oceanic sources, sinks, and transport of atmospheric CO_2, *Global Biogeochem. Cycles*, *23*, GB1005, doi:10.1029/2008GB003349.

Gypens, N., C. Lancelot, and A. V. Borges (2004), Carbon dynamics and CO_2 air-sea exchanges in the eutrophied coastal waters of the Southern Bight of the North Sea: A modelling study, *Biogeosciences*, *1*(2), 147–157, doi:10.5194/bg-1-147-2004.

Hamm, C. E., D. A. Simson, R. Merkel, and V. Smetacek (1999), Colonies of *Phaeocystis globosa* are protected by a thin but tough skin, *Mar. Ecol. Prog. Ser.*, *187*, 101–111, doi:10.3354/meps187101.

Hong, Y., W. O. Smith, and A. M. White (1997), Studies on transparent exopolymer particles (TEP) produced in the Ross Sea (Antarctica) and by *Phaeocystis antarctica* (Prymnesiophyceae), *J. Phycol.*, *33*(3), 368–376, doi:10.1111/j.0022-3646.1997.00368.x.

Jochem, F. J., S. Mathot, and B. Quéguiner (1995), Size-fractionated primary production in the open Southern Ocean in austral spring, *Polar Biol.*, *15*(6), 381–392, doi:10.1007/BF00239714.

Key, R. M., A. Kozyr, C. L. Sabine, K. Lee, R. Wanninkhof, J. L. Bullister, R. A. Feely, F. J. Millero, C. Mordy, and T. H. Peng (2004), A global ocean carbon climatology: Results from Global Data Analysis Project (GLODAP), *Global Biogeochem. Cycles*, *18*, GB4031, doi:10.1029/2004GB002247.

Lancelot, C., E. Hannon, S. Becquevort, C. Veth, and H. J. W. De Baar (2000), Modeling phytoplankton blooms and carbon export production in the Southern Ocean: Dominant controls by light and iron in the Atlantic sector in Austral spring 1992, *Deep Sea Res. Part I*, *47*(9), 1621–1662, doi:10.1016/S0967-0637(00)00005-4.

Lancelot, C., Y. Spitz, N. Gypens, K. Ruddick, S. Becquevort, V. Rousseau, G. Lacroix, and G. Billen (2005), Modelling diatom and *Phaeocystis* blooms and nutrient cycles in the Southern Bight of the North Sea: The MIRO model, *Mar. Ecol. Prog. Ser.*, *289*, 63–78, doi:10.3354/meps289063.

Lancelot, C., A. de Montety, H. Goosse, S. Becquevort, V. Schoemann, B. Pasquer, and M. Vancoppenolle (2009), Spatial distribution of the iron supply to phytoplankton in the Southern Ocean: A model study, *Biogeosciences*, *6*(12), 2861–2878, doi:10.5194/bg-6-2861-2009.

Large, W. G., and S. G. Yeager (2004), Diurnal to decadal global forcing for ocean and sea-ice models: The data sets and flux climatologies, *NCAR Tech. Note NCAR/TN-460+STR*, Natl. Cent. for Atmos. Res., Boulder, Colo.

Locarnini, R. A., A. V. Mishonov, J. I. Antonov, T. P. Boyer, and H. E. Garcia (2006), *World Ocean Atlas 2005*, vol. 1, *Temperature*, *NOAA Atlas NESDIS*, vol. 61, edited by S. Levitus, 182 pp., Silver Spring, Md.

Luo, C., N. M. Mahowald, and J. del Corral (2003), Sensitivity study of meteorological parameters on mineral aerosol mobilization, transport, and distribution, *J. Geophys. Res.*, *108*(D15), 4447, doi:10.1029/2003JD003483.

Mangoni, O., M. Modigh, F. Conversano, G. C. Carrada, and V. Saggiomo (2004), Effects of summer ice coverage on phytoplankton assemblages in the Ross Sea, Antarctica, *Deep Sea Res. Part I*, *51*(11), 1601–1617, doi:10.1016/j.dsr.2004.07.006.

Mathot, S., W. O. Smith Jr., C. A. Carlson, D. L. Garrison, M. M. Gowing, and C. L. Vickers (2000), Carbon partitioning within *Phaeocystis antarctica* (Prymnesiophyceae) colonies in the Ross Sea, Antarctica, *J. Phycol.*, *36*(6), 1049–1056, doi:10.1046/j.1529-8817.2000.99078.x.

Matrai, P. A., M. Vernet, R. Hood, A. Jennings, E. Brody, and S. Saemundsdóttir (1995), Light-dependence of carbon and sulfur production by polar clones of the genus *Phaeocystis*, *Mar. Biol.*, *124*(1), 157–167, doi:10.1007/BF00349157.

Mongin, M., D. M. Nelson, P. Pondaven, and P. Tréguer (2007), Potential phytoplankton responses to iron and stratification changes in the Southern Ocean based on a flexible-composition phytoplankton model, *Global Biogeochem. Cycles*, *21*, GB4020, doi:10.1029/2007GB002972.

Moore, J. K., and O. Braucher (2008), Sedimentary and mineral dust sources of dissolved iron to the world ocean, *Biogeosciences*, *5*(3), 631–656, doi:10.5194/bg-5-631-2008.

Moore, J. K., S. C. Doney, J. A. Kleypas, D. M. Glover, and I. Y. Fung (2002), An intermediate complexity marine ecosystem model for the global domain, *Deep Sea Res. Part II*, *49*(1–3), 403–462, doi:10.1016/S0967-0645(01)00108-4.

Moore, J. K., S. C. Doney, and K. Lindsay (2004), Upper ocean ecosystem dynamics and iron cycling in a global three-dimensional model, *Global Biogeochem. Cycles*, *18*, GB4028, doi:10.1029/2004GB002220.

Moore, C. M., A. E. Hickman, A. J. Poulton, S. Seeyave, and M. I. Lucas (2007), Iron-light interactions during the Crozet Natural Iron Bloom and Export Experiment (CROZEX): Part II—Taxonomic responses and elemental stoichiometry, *Deep Sea Res. Part II*, *54*(18–20), 2066–2084, doi:10.1016/j.dsr2.2007.06.015.

Nejstgaard, J., K. Tang, M. Steinke, J. Dutz, M. Koski, E. Antajan, and J. Long (2007), Zooplankton grazing on *Phaeocystis*: A quantitative review and future challenges, *Biogeochemistry*, *83*(1–3), 147–172, doi:10.1007/s10533-007-9098-y.

Palmisano, A. C., J. B. SooHoo, S. L. SooHoo, S. T. Kottmeier, L. L. Craft, and C. W. Sullivan (1986), Photoadaptation in *Phaeocystis pouchetii* advected beneath annual sea ice in McMurdo Sound, Antarctica, *J. Plankton Res.*, *8*(5), 891–906, doi:10.1093/plankt/8.5.891.

Pasquer, B., G. Laruelle, S. Becquevort, V. Schoemann, H. Goosse, and C. Lancelot (2005), Linking ocean biogeochemical cycles and ecosystem structure and function: Results of the complex SWAMCO-4 model, *J. Sea Res.*, *53*(1–2), 93–108, doi:10.1016/j.seares.2004.07.001.

Peloquin, J. A., and W. O. Smith Jr. (2007), Phytoplankton blooms in the Ross Sea, Antarctica: Interannual variability in magnitude, temporal patterns, and composition, *J. Geophys. Res.*, *112*, C08013, doi:10.1029/2006JC003816.

Poulton, A. J., C. Mark Moore, S. Seeyave, M. I. Lucas, S. Fielding, and P. Ward (2007), Phytoplankton community composition around the Crozet Plateau, with emphasis on diatoms and *Phaeocystis*, *Deep Sea Res. Part II*, *54*(18–20), 2085–2105, doi:10.1016/j.dsr2.2007.06.005.

Rousseau, V., D. Vaulot, R. Casotti, V. Cariou, J. Lenz, J. Gunkel, and M. Baumann (1994), The life cycle of *Phaeocystis* (Prymnesiophycaea): Evidence and hypotheses, *J. Mar. Syst.*, *5*(1), 23–39, doi:10.1016/0924-7963(94)90014-0.

Rousseau, V., S. Becquevort, J. Y. Parent, S. Gasparini, M. H. Daro, M. Tackx, and C. Lancelot (2000), Trophic efficiency of the planktonic food web in a coastal ecosystem dominated by Phaeocystis colonies, *J. Sea Res.*, *43*(3–4), 357–372, doi:10.1016/S1385-1101(00)00018-6.

Sabine, C. L., et al. (2004), The oceanic sink for anthropogenic CO_2, *Science*, *305*(5682), 367–371, doi:10.1126/science.1097403.

Saito, M. A., and T. J. Goepfert (2008), Zinc-cobalt colimitation of *Phaeocystis antarctica*, *Limnol. Oceanogr.*, *53*(1), 266–275, doi:10.4319/lo.2008.53.1.0266.

Schoemann, V., S. Becquevort, J. Stefels, V. Rousseau, and C. Lancelot (2005), Phaeocystis blooms in the global ocean and their controlling mechanisms: A review, *J. Sea Res.*, *53*(1–2), 43–66, doi:10.1016/j.seares.2004.01.008.

Sedwick, P., N. Garcia, S. Riseman, C. Marsay, and G. DiTullio (2007), Evidence for high iron requirements of colonial *Phaeocystis antarctica* at low irradiance, *Biogeochemistry*, *83*(1–3), 83–97, doi:10.1007/s10533-007-9081-7.

Shields, A. R., and W. O. Smith (2009), Size-fractionated photosynthesis/irradiance relationships during *Phaeocystis antarctica*-dominated blooms in the Ross Sea, Antarctica, *J. Plankton Res.*, *31*(7), 701–712, doi:10.1093/plankt/fbp022

Smith, W. O., Jr., and V. L. Asper (2001), The influence of phytoplankton assemblage composition on biogeochemical characteristics and cycles in the southern Ross Sea, Antarctica, *Deep Sea Res. Part I*, *48*(1), 137–161, doi:10.1016/S0967-0637(00)00045-5.

Smith, W. O., Jr., D. Nelson, and S. Mathot (1999), Phytoplankton growth rates in the Ross Sea, Antarctica, determined by independent methods: Temporal variations, *J. Plankton Res.*, *21*(8), 1519–1536, doi:10.1093/plankt/21.8.1519.

Solomon, C. M., E. J. Lessard, R. G. Keil, and M. S. Foy (2003), Characterization of extracellular polymers of *Phaeocystis globosa* and *P. antarctica*, *Mar. Ecol. Prog. Ser.*, *250*, 81–89, doi:10.3354/meps250081.

Tagliabue, A., and K. R. Arrigo (2003), Anomalously low zooplankton abundance in the Ross Sea: An alternative explanation, *Limnol. Oceanogr.*, *48*(2), 686–699, doi:10.4319/lo.2003.48.2.0686.

Tagliabue, A., and K. R. Arrigo (2005), Iron in the Ross Sea: 1. Impact on CO_2 fluxes via variation in phytoplankton functional group and non-Redfield stoichiometry, *J. Geophys. Res.*, *110*, C03009, doi:10.1029/2004JC002531.

Tagliabue, A., and K. R. Arrigo (2006), Processes governing the supply of iron to phytoplankton in stratified seas, *J. Geophys. Res.*, *111*, C06019, doi:10.1029/2005JC003363.

Takahashi, T., et al. (2002), Global sea-air CO_2 flux based on climatological surface ocean pCO_2, and seasonal biological and temperature effects, *Deep Sea Res. Part II*, *49*(9–10), 1601–1622, doi:10.1016/S0967-0645(02)00003-6.

Tang, K. W., W. O. Smith, A. R. Shields, and D. T. Elliott (2009), Survival and recovery of *Phaeocystis antarctica* (Prymnesiophyceae) from prolonged darkness and freezing, *Proc. R. Soc. London B*, *276*(1654), 81–90, doi:10.1098/rspb.2008.0598.

Taylor, K. E. (2001), Summarizing multiple aspects of model performance in a single diagram, *J. Geophys. Res.*, *106*(D7), 7183–7192, doi:10.1029/2000JD900719.

van Hilst, C. M., and W. O. Smith (2002), Photosynthesis/irradiance relationships in the Ross Sea, Antarctica, and their control by phytoplankton

assemblage composition and environmental factors, *Mar. Ecol. Prog. Ser.*, *226*, 1–12, doi:10.3354/meps226001.

van Leeuwe, M. A., and J. Stefels (1998), Effects of iron and light stress on the biochemical composition of Antarctic *Phaeocystis sp.* (Prymnesiophyceae). Part II. Pigment composition, *J. Phycol.*, *34*(3), 496–503, doi:10.1046/j.1529-8817.1998.340496.x.

Veldhuis, M. J. W., C. P. D. Brussaard, and A. A. M. Noordeloos (2005), Living in a *Phaeocystis* colony: A way to be a successful algal species, *Harmful Algae*, *4*(5), 841–858, doi:10.1016/j.hal.2004.12.013.

Weber, L. H., and S. Z. El-Sayed (1987), Contributions of the net, nano- and picoplankton to the phytoplankton standing crop and primary productivity in the Southern Ocean, *J. Plankton Res.*, *9*(5), 973–994, doi:10.1093/plankt/9.5.973.

Worthen, D. L., and K. R. Arrigo (2004), A coupled ocean-ecosystem model of the Ross Sea: 1. Interannual variability of primary production and phytoplankton community structure, in *Biogeochemistry of the Ross Sea*, *Antarct. Res. Ser.*, vol. 78, edited by G. R. DiTullio and R. B. Dunbar, pp. 93–106, AGU, Washington, D. C.

Yeager, S. G., C. A. Shields, W. G. Large, and J. J. Hack (2006), The low-resolution CCSM3, *J. Clim.*, *19*(11), 2545–2566, doi:10.1175/JCLI3744.1.

J. K. Moore and S. Wang, Department of Earth System Science, University of California, Irvine, CA 92697, USA. (shanlinw@uci.edu)